THE LONG-TERM EFFECT OF EARTHQUAKES: USING GEOSPATIAL SOLUTIONS TO EVALUATE HEIGHTENED ROCKFALL ACTIVITY ON CRITICAL LIFELINES

FINAL PROJECT REPORT

by

Margaret M. Darrow
Daisy M. Herrman
University of Alaska Fairbanks

Kat Holtan
Ben Leshchinsky
Michael Olsen
Oregon State University

Joseph Wartman
University of Washington

Sponsorship
Oregon Department of Transportation, University of Alaska Fairbanks,
University of Washington

for

Pacific Northwest Transportation Consortium (PacTrans)
USDOT University Transportation Center for Federal Region 10
University of Washington
More Hall 112, Box 352700
Seattle, WA 98195-2700

In cooperation with U.S. Department of Transportation,
Office of the Assistant Secretary for Research and Technology (OST-R)

DISCLAIMER

The contents of this report reflect the views of the authors, who are responsible for the facts and the accuracy of the information presented herein. This document is disseminated under the sponsorship of the U.S. Department of Transportation's University Transportation Centers Program, in the interest of information exchange. The Pacific Northwest Transportation Consortium, the U.S. Government and matching sponsor assume no liability for the contents or use thereof.

TECHNICAL REPORT DOCUMENTATION PAGE

1. Report No.	2. Government Accession No.	3. Recipient's Catalog No.
	01763326	

4. Title and Subtitle	5. Report Date
THE LONG-TERM EFFECT OF EARTHQUAKES: USING GEOSPATIAL SOLUTIONS TO EVALUATE HEIGHTENED ROCKFALL ACTIVITY ON CRITICAL LIFELINES	11/7/2022
	6. Performing Organization Code
7. Author(s) and Affiliations	**8. Performing Organization Report No.**
Margaret M. Darrow, 0000-0003-4078-4746; Daisy M. Herrman; University of Alaska Fairbanks Kat Holtan, Ben Leshchinsky, 0000-0003-3890-1368; Michael Olsen, 0000-0002-2989-5309; Oregon State University Joseph Wartman; 0000-0001-7659-7198; University of Washington	2020-M-UAF-2
9. Performing Organization Name and Address	**10. Work Unit No. (TRAIS)**
PacTrans Pacific Northwest Transportation Consortium University Transportation Center for Federal Region 10 University of Washington More Hall 112 Seattle, WA 98195-2700	**11. Contract or Grant No.** 69A3551747110
12. Sponsoring Organization Name and Address	**13. Type of Report and Period Covered**
United States Department of Transportation Research and Innovative Technology Administration 1200 New Jersey Avenue, SE Washington, DC 20590	Research, 8/15/2020-2/15/2023 **14. Sponsoring Agency Code**

15. Supplementary Notes

Report uploaded to: www.pactrans.org

16. Abstract

Rockfall is a chronic slope hazard along transportation corridors throughout the Pacific Northwest (PNW), resulting in frequent road closures and lane restrictions, and directly impacting driver safety, mobility, and accessibility for many critical lifelines. These impacts are amplified by moderate- to large-magnitude seismic events – both during and after shaking, making earthquakes a driver of persistent rockfall hazards. For this project, we performed continued monitoring of rockfall activity on a series of rock slopes via repeat terrestrial laser scanning, geologic characterization, and imagery collection. These data, as well as custom-generated shakemaps and a database creation (Alaska GAM, ODOT unstable slopes database) of rockfall events throughout the PNW and New Zealand, enable extrapolation of potential coseismic and post-seismic hazards to a variety of earthquake scenarios in Alaska. We extend and modify the Rockfall Activity Rate System (RoARS) model to rock slope sites in two Alaskan transportation corridors to evaluate coseismic and post-seismic rockfall hazard at a regional scale, as well as estimate rockfall volumes and associated closure times. We find that both corridors are prone to earthquake-induced rockfall activity, but the magnitude and long-term persistence of this activity is highly dependent on the given rupture event, as are closure times along each corridor. While scenario-dependent, this database and model creation explores a new avenue for decision-makers to evaluate potential rockfall scenarios considering seismic disturbance, and consequently, plan accordingly for closures and restoration of mobility following shaking.

17. Key Words	18. Distribution Statement		
Rockfalls, laser radar, lane closure, earthquakes, Alaska			
19. Security Classification (of this report)	**20. Security Classification (of this page)**	**21. No. of Pages**	**22. Price**
Unclassified.	Unclassified.	74	N/A

Form DOT F 1700.7 (8-72) **Reproduction of completed page authorized.**

SI* (MODERN METRIC) CONVERSION FACTORS

APPROXIMATE CONVERSIONS TO SI UNITS				
Symbol	**When You Know**	**Multiply By**	**To Find**	**Symbol**
		LENGTH		
in	inches	25.4	millimeters	mm
ft	feet	0.305	meters	m
yd	yards	0.914	meters	m
mi	miles	1.61	kilometers	km
		AREA		
in^2	square inches	645.2	square millimeters	mm^2
ft^2	square feet	0.093	square meters	m^2
yd^2	square yard	0.836	square meters	m^2
ac	acres	0.405	hectares	ha
mi^2	square miles	2.59	square kilometers	km^2
		VOLUME		
fl oz	fluid ounces	29.57	milliliters	mL
gal	gallons	3.785	liters	L
ft^3	cubic feet	0.028	cubic meters	m^3
yd^3	cubic yards	0.765	cubic meters	m^3
		NOTE: volumes greater than 1000 L shall be shown in m^3		
		MASS		
oz	ounces	28.35	grams	g
lb	pounds	0.454	kilograms	kg
T	short tons (2000 lb)	0.907	megagrams (or "metric ton")	Mg (or "t")
		TEMPERATURE (exact degrees)		
°F	Fahrenheit	5 (F-32)/9 or (F-32)/1.8	Celsius	°C
		ILLUMINATION		
fc	foot-candles	10.76	lux	lx
fl	foot-Lamberts	3.426	candela/m^2	cd/m^2
		FORCE and PRESSURE or STRESS		
lbf	poundforce	4.45	newtons	N
lbf/in^2	poundforce per square inch	6.89	kilopascals	kPa

APPROXIMATE CONVERSIONS FROM SI UNITS				
Symbol	**When You Know**	**Multiply By**	**To Find**	**Symbol**
		LENGTH		
mm	millimeters	0.039	inches	in
m	meters	3.28	feet	ft
m	meters	1.09	yards	yd
km	kilometers	0.621	miles	mi
		AREA		
mm^2	square millimeters	0.0016	square inches	in^2
m^2	square meters	10.764	square feet	ft^2
m^2	square meters	1.195	square yards	yd^2
ha	hectares	2.47	acres	ac
km^2	square kilometers	0.386	square miles	mi^2
		VOLUME		
mL	milliliters	0.034	fluid ounces	fl oz
L	liters	0.264	gallons	gal
m^3	cubic meters	35.314	cubic feet	ft^3
m^3	cubic meters	1.307	cubic yards	yd^3
		MASS		
g	grams	0.035	ounces	oz
kg	kilograms	2.202	pounds	lb
Mg (or "t")	megagrams (or "metric ton")	1.103	short tons (2000 lb)	T
		TEMPERATURE (exact degrees)		
°C	Celsius	1.8C+32	Fahrenheit	°F
		ILLUMINATION		
lx	lux	0.0929	foot-candles	fc
cd/m^2	candela/m^2	0.2919	foot-Lamberts	fl
		FORCE and PRESSURE or STRESS		
N	newtons	0.225	poundforce	lbf
kPa	kilopascals	0.145	poundforce per square inch	lbf/in^2

*SI is the symbol for the International System of Units. Appropriate rounding should be made to comply with Section 4 of ASTM E380.
(Revised March 2003)

TABLE OF CONTENTS

LIST OF FIGURES

LIST OF TABLES

LIST OF ABBREVIATIONS

AADT	Average annual daily traffic
ADOT&PF	Alaska Department of Transportation and Public Facilities
AEC	Alaska Earthquake Center
AFB	Airforce Base
AOI	Area of interest
CES	Canterbury New Zealand Earthquake Sequence
DTMs	Digital terrain models
EHP	Earthquake Hazards Program
EQ	Earthquake
FEMA	Federal Emergency Management Agency
GAM	Geotechnical Asset Management
GDB	Geodatabase
GIS	Geographic Information System
IF	Increase Factor
LL	Long Lake
MP	Milepost
M_w	Moment magnitude
NEQ	Non-earthquake
NNW	North-northwest
NSF	National Science Foundation
ODOT	Oregon Department of Transportation
PacTrans	Pacific Northwest Transportation Consortium
PNW	Pacific Northwest
PGA	Peak ground acceleration
RAI	Rockfall Activity Index
RAI_{eq}	Post-Seismic Rockfall Activity Index
RAPID	NSF Rapid Response Research grant
RIMs	Rockfall Impacts to Mobility database
RoARS	Rockfall Activity Rate System
SC	Scenario
SH	Schmidt hammer
TLS	Terrestrial lidar scanning
UAS	Unmanned aircraft systems
USGS	United States Geological Survey
WBZ	Wadati-Benioff Zone
WSDOT	Washington State Department of Transportation

ACKNOWLEDGMENTS

The authors thank many individuals with the Alaska Department of Transportation and Public Facilities for helping to facilitate the field work and providing access to the rockfall inventory database. We also thank Drs. Michael West, Matt Gardine, Natalia Ruppert, and Carl Tape from the Alaska Earthquake Center for creating the scenario shakemaps, and Dr. Chris Massey with GNS Science for the support with the RoARS framework. We thank Leica Geosystems, David Evans and Associates, and Maptek I-Site for providing hardware and software used for the terrestrial laser scan data.

EXECUTIVE SUMMARY

Rockfall is a chronic slope hazard along transportation corridors throughout the Pacific Northwest (PNW), resulting in frequent road closures and lane restrictions, directly impacting driver safety, mobility, and accessibility for many critical lifelines. These impacts are amplified by moderate- to large-magnitude seismic events — both during *and* after shaking, making earthquakes a driver of persistent rockfall hazards. For this project, we performed continued monitoring of rockfall activity on a series of rock slopes via repeat terrestrial laser scanning, geologic characterization, and imagery acquisition. These efforts included a series of rock slopes subjected to seismic disturbance from the 2018 Anchorage Earthquake, where both pre-seismic, coseismic, and post-seismic rockfall activity is constrained. These data, along with compiling various rockfall events throughout the PNW and New Zealand into a comprehensive database, serves as a basis for creating predictive models to evaluate post-seismic rockfall hazard.

At both the Nenana Canyon (aka, Glitter Gulch (GG)) and Long Lake (LL) rock slope sites, terrestrial laser scanning (TLS) data was collected, reflecting the eleventh dataset for the sites, and eight years of continued rockfall monitoring. Further, we performed geological site characterization, including measurement of discontinuity/joint/bedding attitude as well as lithology to supplement further interpretation of controls on rock slope failure. Geological characterization of each rock slope reveals that both GG and LL sites have different geologic controls on instability, but both sets of rock slopes are still predisposed to elevated rockfall activity. Analysis of change from TLS data reveals that both sets of rock slopes are highly active in rockfall activity. While this activity is variable from year to year, overhanging and fractured portions of rock slopes are prone to more frequent and larger rockfall. While the GG sites did not experience significant shaking from the 2018 Anchorage Earthquake, the LL sites did experience modest shaking (~0.10g). A notable uptick in rockfall activity is observed following the earthquake at LL71. Higher frequency data collection following the earthquake indicates that much of this rockfall activity is largely post-seismic, although there was presumably a modest evacuation of rock slope material from shaking itself. There is an observed decay in rockfall activity that lasts at least two years when excluding a singular large rockfall event prior to the earthquake.

These data, as well as custom-generated shakemaps and a database creation (Alaska GAM, ODOT unstable slopes database) of rockfall events throughout the PNW and New Zealand enable extrapolation of potential coseismic and post-seismic hazards to a variety of earthquake scenarios in Alaska. We extend and modify the RoARS model to LL and GG rock slope sites to evaluate coseismic and post-seismic rockfall hazard at a regional scale, as well as estimate rockfall volumes and associate closure times. We find that both corridors are prone to earthquake-induced rockfall activity, but the magnitude and long-term persistence of this activity is highly dependent on the given rupture event, as are closure times along each corridor. While scenario-dependent, this database and model creation explores a new avenue for decision-makers to evaluate potential rockfall scenarios considering seismic disturbance, and consequently, plan accordingly for closures and restoration of mobility following shaking.

CHAPTER 1. PROJECT MOTIVATION AND BACKGROUND

1.1. Introduction

Rockfall is a chronic slope hazard along transportation corridors throughout North America, where tens of millions of dollars are spent annually on rock slope maintenance and mitigation works (Turner and Schuster 2012). The problem is particularly acute throughout much of the Pacific Northwest (PNW). In this region, the combination of topographic relief, high rates of precipitation, and elevated seismicity create a setting where rockfall is widespread and pervasive. Rockfall hazards result in frequent road closures and lane restrictions, damage to infrastructure, and loss-of-life and injuries to motorists, cyclists, and pedestrians. Thus, rockfall directly impacts driver safety, mobility, and accessibility for many critical lifelines across the PNW. These impacts are amplified by moderate- to large-magnitude seismic events — both during *and* long after shaking. Seismic activity poses one of the most significant threats to nearly all parts of the PNW (Goldfinger et al. 2012, Frankel et al. 2018). Moreover, it has been shown that earthquakes may dramatically increase rockfall activity (Massey et al. 2014), both during shaking and the months and years after an earthquake. One example is the 30 November 2018 Anchorage, Alaska earthquake, which resulted in significant traffic delays while debris and damaged vehicles were removed. These events create and pose significant life safety concerns during and immediately after an earthquake as stalled motorists are trapped adjacent to precarious rock slopes while aftershocks continue to occur after the main event. Rockfall hazards, however, do not end after an earthquake; increased rates of rockfall may negatively impact mobility and safety long after strong shaking (and major aftershocks) end. Further complexity is added when an earthquake occurs during or after periods of increased levels and intensity of precipitation.

Unfortunately, there is a relatively limited understanding of the effects of large earthquakes on subsequent rockfall activity. Following the 2018 Anchorage earthquake, members of our research team secured a small "rapid response" research grant from the National Science Foundation (NSF) to deploy to Alaska in the aftermath of the event to collect highly perishable data on the post-seismic response of select rock slopes that were strongly shaken and, serendipitously, were part of previous PacTrans studies. For the research presented here, we analyzed these data to answer the following research questions: (1) What was the “baseline” rockfall activity at the study sites, and how did this vary (if at all) with fluctuations in local climate conditions?; (2) What are the mechanisms and factors that govern rockfall both during and after the event; how, if at all, do these vary from the pre-earthquake activity?; (3) How soon after the earthquake does rockfall activity and magnitude return to baseline conditions?; and (4) How is this influenced by short-term local weather conditions during this period of “recovery”? Answering these questions is critical for transportation agencies to plan for and allocate resources optimally to address maintenance needs for rock debris removal and slope mitigation, thus ensuring efficient mobility of the transportation network. In cases where rockfall occurs in mountainous terrain along highways, road closure means *several hours of delay* as motorists must take much longer alternate routes given the limited options available in these areas.

Answers to these questions also will enable the development of practice-oriented seismic rockfall stability guidelines and predictive tools. Specifically, the Rockfall Activity Index (RAI) — a detailed hazard assessment system developed in a prior PacTrans project (Dunham et al. 2017) — has recently been modified in a research project for Oregon DOT to identify hazards and performance under seismic and post-seismic conditions ("RAI_{eq}"); however, when developing this model, there was virtually no empirical data available from sites with both baseline and post-seismic lidar scans to validate the RAI_{eq} model. In addition to the RAI_{eq}, which provides a detailed analysis of a rock slope site, a Rockfall Activity Rate System (RoARS) was developed, which is a simplified system developed to estimate the volume increase and time to restoration of rock slopes for seismic events along a highway corridor. The data available before and after the 2018 seismic event in Alaska provide a rare and extraordinary opportunity to validate, refine, and enhance these models based on high-quality field information, providing a data-driven solution for planners who must ensure mobility and driver safety in the PNW, during and after seismic events. Additionally, the proposed analysis of a post-earthquake dataset will enable a significantly improved understanding of seismic and post-seismic rockfall processes, and more pragmatically, how this affects the rate of rockfall activity over long time periods. These data will directly expand the capabilities and validate the basis of RAI and RoARS for coseismic (i.e., during shaking) and post-seismic failures.

This research benefits mobility and safety by (1) providing data-driven tools and analyses for understanding which rock slopes may show heightened rockfall activity, and (2) establishing a quantitative basis for assessing safety risks to motorists and others exposed to rockfall during earthquake recovery. A better understanding of rock slope response enables an improved approach for enhanced mobility, safety, and commerce.

1.2. Background

Earthquakes often trigger significant rockfall activity along steep cliffs. This activity may linger for an extended period of time after shaking, owing to the weakening of rock slope materials, such as fractures (e.g., Massey et al. 2014, Olsen et al. 2019, Olsen et al. 2020, and Massey et al. 2022). In November 2018, Anchorage, Alaska experienced a strong earthquake (up to 0.4g) that resulted in numerous ground failures, including rockfalls, landslides, and lateral spreads. The combination of potentially large volumes, high velocities, long travel distances, and impact forces make rockfall hazard significant to motorists. Based on observations from past events, such as the Canterbury Earthquake Sequence and Kaikoura in New Zealand (Massey et al. 2014), rockfall activity exceeds “normal” baseline levels before diminishing over a period of several months to years (Figure 1.1). Because the slopes are weakened, slope failures are more prevalent and damaging, especially during storm events in the years following significant seismic activity. This heightened rockfall activity affects transportation safety, maintenance frequency, supply chain logistics, and resource allotment during the critical period following an earthquake event (e.g., Mason et al. 2017). As these lingering influences are often overshadowed by concerns resulting from the actual shaking, these long-term effects can potentially impart costs and impacts that meet or exceed the same impacts due to shaking because they occur over a much longer time scale. While this post-seismic recovery stage is critical, to the best of our knowledge, *no prior study of seismic rockfall activity and recovery has had the benefit of accurate, detailed baseline rockfall activity information prior to the event*. Rockfall rates must be estimated from laborious field campaigns that result in a high level of uncertainty given that much material has long been removed, particularly in locations along highways where work needs to be completed quickly to reopen the highway. Fortuitously, we collected baseline data for several years prior to the 2018 Anchorage earthquake. This valuable and rare “baseline” multi-year dataset provides a unique opportunity to understand the magnitude and timescale of the disturbance incurred from the 2018 earthquake on a series of impacted rock slopes.

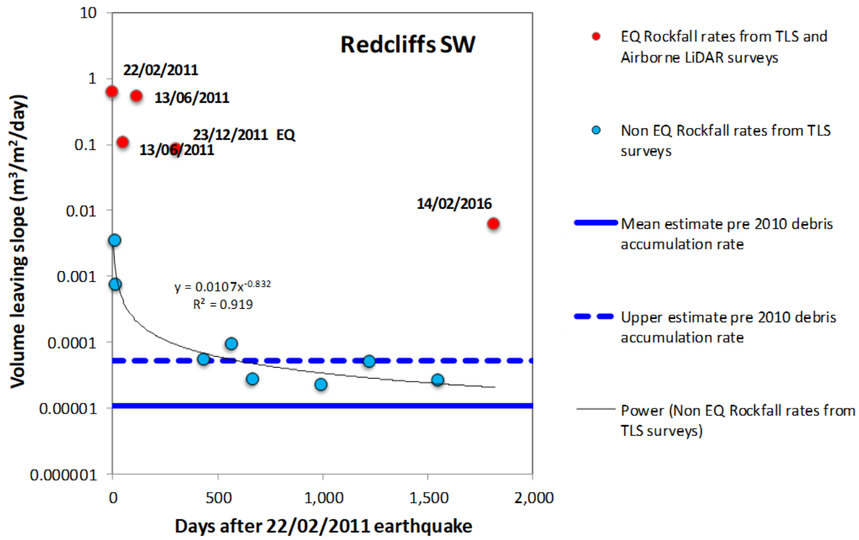

Figure 1.1 Earthquake (EQ) and non-earthquake (Non-EQ) rockfall rates from terrestrial laser scan (TLS) and airborne lidar surveys. The pre-2010 debris accumulation rates (mean and upper estimates) are estimated from dating surfaces on top of which pre-2010 debris – debris present before the start of the 2010/11 Canterbury earthquake sequence – from the slopes lie (modified from Litchfield et al. 2016).

The recent Canterbury, New Zealand Earthquake Sequence triggered many thousands of rockfalls, which resulted in the unfortunate loss of life and significantly damaged motorways, residential dwellings, and commercial structures. Detailed 3D terrestrial lidar scan surveys were periodically collected at several rock slope sites throughout the Port Hills in Christchurch, New Zealand, to document the rockfall activity as well as assess the post-earthquake stability of the slopes. This dataset spans five years of seismic activity that includes several large earthquakes but lacks critical pre-event baseline data. Analysis of this dataset indicates that the activity rates and volume of material leaving the cliff occurred at heightened levels following shaking and decayed with time. Through regression analyses based on correlating volume loss observed in New Zealand with readily obtainable variables of slope height, slope angle, geomorphic erosion rates, and peak ground acceleration (PGA), a rapid forecasting system called the RoARS was developed by the research team (Olsen et al. 2020, Massey et al. 2022). As an example, RoARS was applied along a highway corridor in Oregon, U.S.A. to predict the potential increases in rockfall activity and volumes resulting from a major earthquake as well as an estimate of the time to return to baseline conditions for rockfall activity (Figure 1.1). This information was provided in a geographic information system (GIS) framework (Figure 1.2), which subsequently can be integrated into transportation network analysis to predict the economic and environmental impacts resulting from mobility loss due to partial or full highway closures at these locations due to increased rockfall activity.

In this same study, the U.S.-New Zealand research team also formulated a modified version of the RAI (Dunham et al. 2017) to capture the increase in both activity rates and size (i.e., volume) of rockfall events following earthquakes. The modified version of the RAI, referred to herein as "RAI_{eq}," differs from RoARS in that it provides a localized, high-resolution (cm-scale) mapping of potential rockfall hotspots across a slope face, and thus may be directly used to support post-event mitigation interventions (e.g., localized scaling) and risk assessment (Olsen et al., 2020). DOTs also can use both the RAI_{eq} and RoARS systems with FEMA funding requests to determine the increase in maintenance personnel

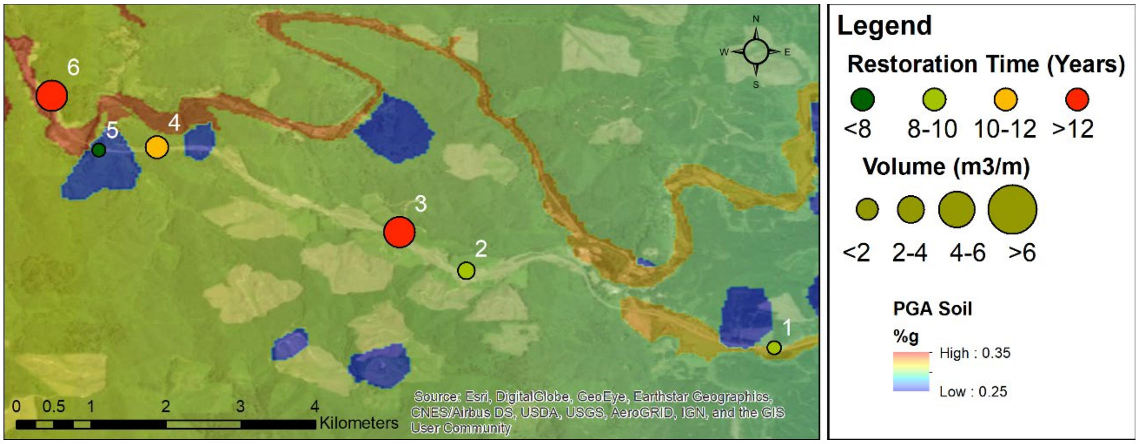

Figure 1.2 Example results of rockfall analysis along the US20 Highway Corridor near Eddyville, Oregon, showing differences in the amounts of anticipated rockfall from an earthquake and time to restoration. A transparent PGA basemap is over an aerial photograph. Note that the high PGA values follow alluvial material along the river, which amplifies the seismic signals compared with bedrock

required to keep highways clear of debris so that traffic can continue to travel these corridors with minimal delays. The models were conceptualized based on data from the Port Hills region of New Zealand during the Christchurch Earthquake sequence of 2010-2011. These lidar data are valuable, but lack a pre-event baseline dataset to understand pre-event conditions and to forecast when activity returns to baseline levels. By using and comparing both our PacTrans pre-event terrestrial lidar dataset and the post-event data collected in the NSF rapid response project, we can refine, calibrate, and validate RAI_{eq}.

1.3. Research Approach and Report Structure

This project consisted of the following tasks. The report chapter/s that address results of each task is/are indicated in italics and parentheses.

Task 1 ***(****Error! Reference source not found.**)***: Collect additional datasets of terrestrial laser scanning and unmanned aircraft systems (UAS) structure from motion/multi-view stereo photogrammetry at two Alaska sites (Figure 1.3) to capture effects after shaking.

Task 2 ***(CHAPTER 2)*****:** Conduct a site characterization of each field site to map local bedrock geology, and to determine rock strength through field tests.

Task 3 ***(CHAPTER 3)*****:** Analyze the previously-collected post-seismic datasets to evaluate rockfall activity rate trends post-earthquake at the Long Lake site.

Task 4 ***(CHAPTER 4)*****:** Develop a process to extract slope metrics (height and angles) efficiently from mobile or airborne lidar data collected along long sections of highways to provide the necessary GIS input to RoARS. Develop a python script and supporting toolbox to implement RoARS in a GIS framework.

Task 5 ***(CHAPTER 4)*****:** Apply the process and scripts developed in Task 4 to the rock slopes located within two 10-mile segments where mobile or airborne lidar are available to estimate post-seismic rockfall trends.

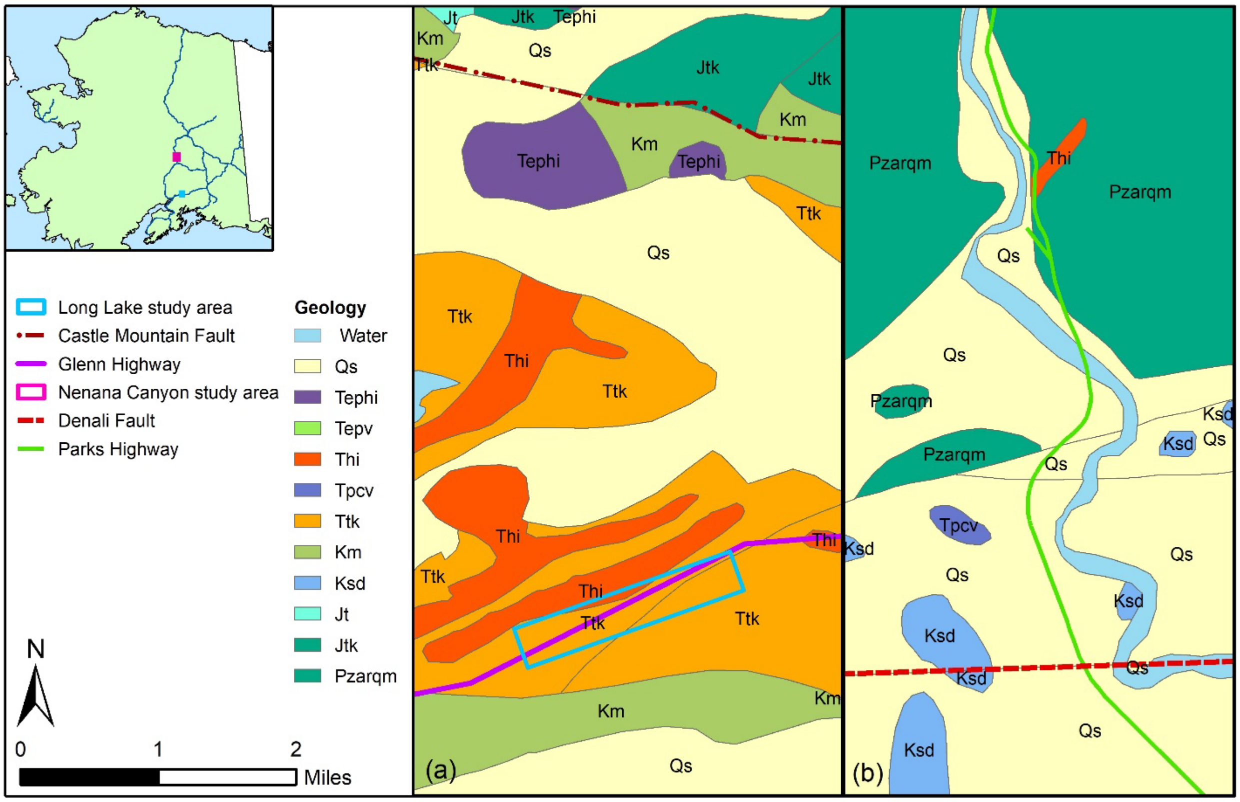

Figure 1.3 Location and bedrock geology maps for the (a) Long Lake and (b) Nenana Canyon research locations. Inset of Alaska Indicates location of (a) in light blue and (b) in pink, along with distribution of major roads in the state. (Base map data from AGC 2020, and Wilson et al. 2015).

Task 6 *(CHAPTER 3)*: Refine and validate the RAIeq model. Assess and statistically analyze the post-earthquake lidar datasets for the strongly-shaken sites on the Glenn Highway (notably, MP 71) to quantify the increase in activity and size of rockfall events for each RAI morphological class following the earthquake.

Task 7 *(CHAPTER 4)*: Use the Rockfall Impacts to Mobility database (RIM) under development in a current PacTrans project to estimate closure and delay times along those sections of highways considering coseismic and post-seismic rockfall events.

Chapter 5 presents a summary and our conclusions. The appendix contains the python code developed for the regional seismic analysis.

CHAPTER 2. SITE CHARACTERIZATIONS

2.1. Methods

In September 2020, we collected terrestrial lidar data using a Maptek LR3 with a pair of Leica GS14s for georeferencing (base and rover); however, because of the COVID-19 pandemic, only the Alaska-based part of the research team consisting of two individuals performed the data collection. Thus, limited Schmidt hammer data were collected, and only a few representative rocks were tested using the field point-load testing device.

For the June 7-13, 2021 field work, travel restrictions had eased, and our team consisted of five members. Similar equipment was used for the terrestrial lidar data. At any given site, two to three individuals collected the lidar data, while the other team members mapped bedrock structural features, made Schmidt hammer measurements, and collected representative rocks from the Schmidt hammer sites for point-load testing. We used "Geopads" to conduct the geologic mapping. Geopads are iPad minis (5th generation) in rugged, waterproof cases, that incorporate a BadElf GPS unit for determining position. We used the FieldMove software to measure orientations of bedding, joints, and faults (see Figure 2.1 for a measurement example). Once back in the office, we used Rocscience Dips to analyze the structural data. For strength measurements, we used two Schmidt hammer devices (Rock Schmidt Rebound Hammer, Type N with impact energy 2.207 Nm (1.63 ft-lbf), and Original Schmidt Test Hammer, Type L with impact energy 0.735 Nm (0.54 ft-lbf)). We typically made measurements in a 1 m^2 area of the rock slope face. We tested rocks collected from the same area of the Schmidt hammer measurements using a portable point load testing device (Wille Geotechnik). All field tests were made following ASTM standards (ASTM 2007, 2014).

Figure 2.1 Measuring orientation of a fault at Long Lake 71 using the Geopad system.

2.2. Glenn Highway / Long Lake Site Descriptions

2.2.1. Long Lake Milepoint (MP) 71

This road cut consists of dark gray mudstone (grain size ranges 1/8-1/4 mm) from the upper Matanuska Formation (Trop et al. 2015). Calcite veins are prominent in some samples, and the rock reacts with hydrochloric acid, supporting its marine origin. On June 8, 2021, we conducted Schmidt hammer (SH) readings using both hammer types at 11 locations. We also collected two sets of readings using the Rock

Schmidt rebound hammer with two different people collecting the measurements, to determine the effect of the individual taking the measurements. Measurements were made perpendicular to bedding. We collected samples of the mudstone at three of the SH testing locations for point-load testing. We also made 95 measurements of discontinuities, including bedding, faults, and joints (Figure 2.1).

The mudstone bedding is nearly vertical, with dip and dip direction of 80° and 140°, respectively (Figure 2.2). The road cut stands up to 47-m high at a 79° maximum slope angle (facing 130°), which roughly parallels the dip of the bedding (Figure 2.3). Other structural features include four sets of faults and/or joints. We observed slickensides along some high-angle fault contacts, which suggested normal faulting as the sense of displacement.

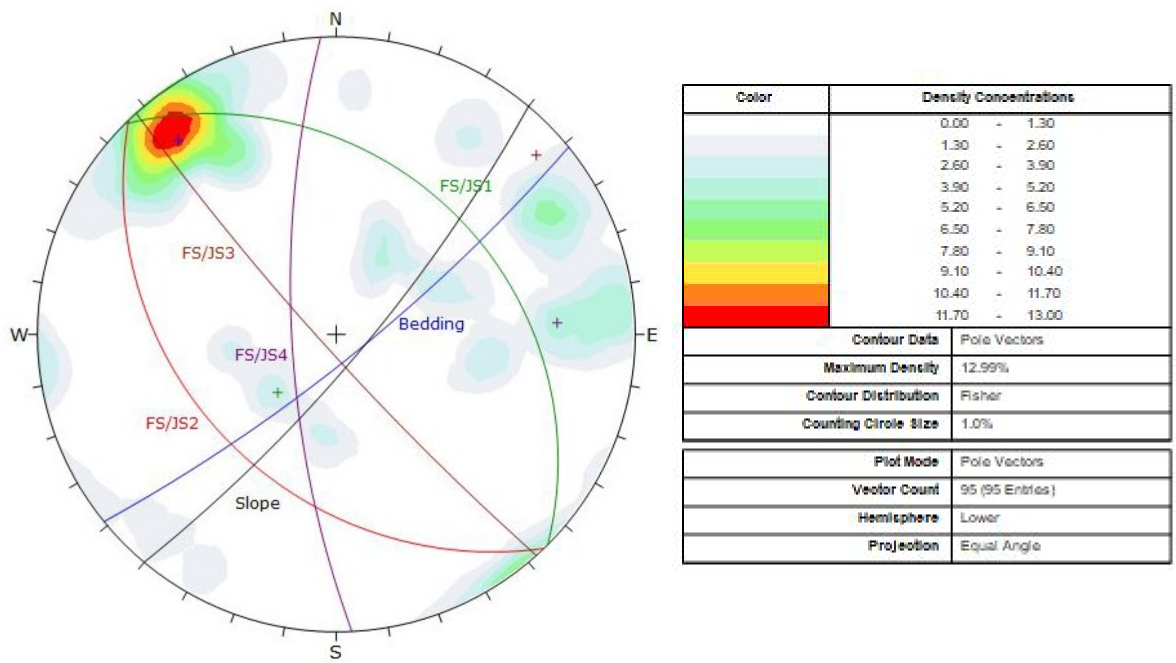

Figure 2.2 Stereonet for Long Lake 71 mudstone.

Figure 2.3 Example of carbonaceous mudstone with steeply-dipping bedding at LL71 site.

2.2.2. Long Lake MP 75.8

This road cut consists of light gray fine- to medium-grained (1/8-1/2 mm) sandstone with interbedded (up to 20-cm thick) carbonaceous mudstone of the Chickaloon Formation (Trop et al. 2015). The sandstone is 60-80% quartz and ~5% plagioclase with other accessory minerals. Some leaf fossils are present in the black, fine-grained mudstone. Bedding is prominent in hand samples, which split easily on the bedding surfaces. Near the western edge of the road cut is a rhyolite-dacite dike/sill. This same rock forms a sill at the eastern edge of the site, and its contact with baked carbonaceous mudstone is visible (Figure 2.4; Trop et al. 2015). The gray porphyritic rhyodacite contains 1-3 mm quartz crystals (60%) and 20-30% plagioclase with other accessory minerals.

On June 7, 2021, we conducted Schmidt hammer testing at five locations, three on sandstone perpendicular to bedding, and two on the rhyodacite. All were tested at 45 degrees up from horizontal. We collected samples of the sandstone and rhyodacite for point load testing. On June 8, 2021, we collected 112 measurements of joints in the rhyodacite (Figure 2.5), and 168 measurements of bedding and joints in the sandstone and mudstone (Figure 2.6). The combination of bedding and jointing make this a site for classic planar failure, with large blocks sliding down the bedding surface. The road cut stands up to 22-m high (facing 130°) at a 66° slope, with both the sandstone and rhyodacite presenting some overhanging areas.

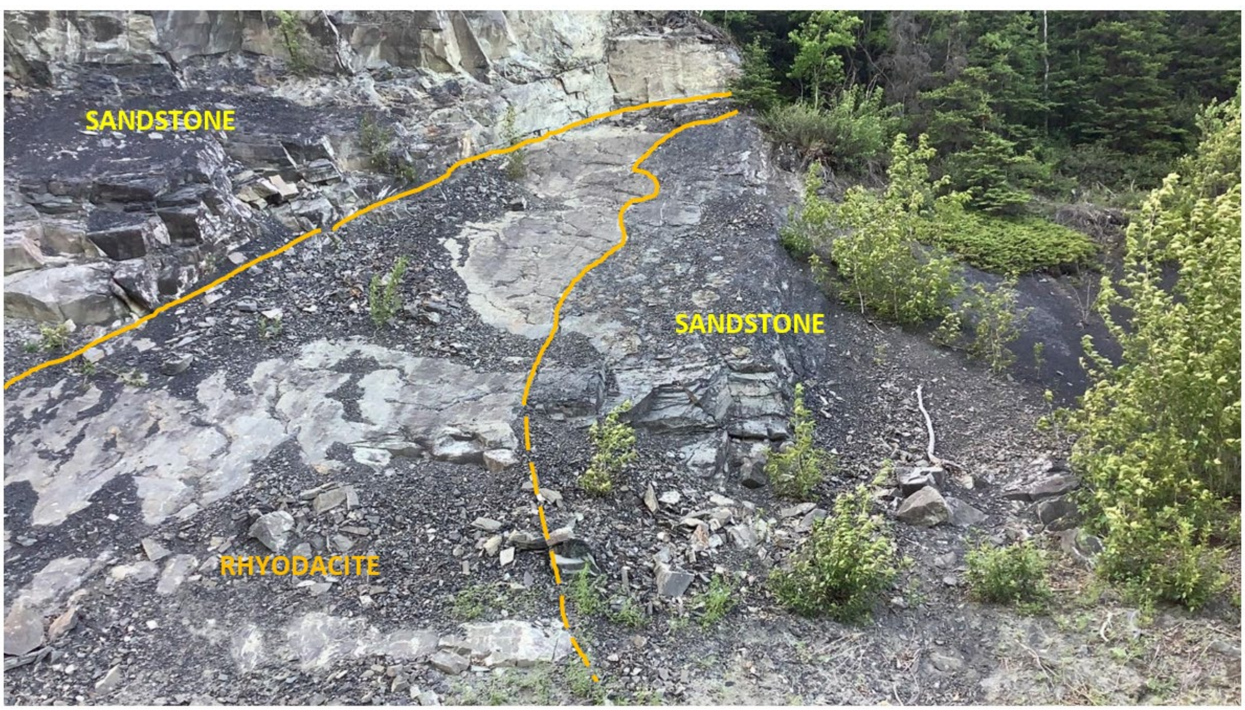

Figure 2.4 Rhyodacite sill intruded into sandstone at eastern end of LL 75.8 site. Contacts are annotated.

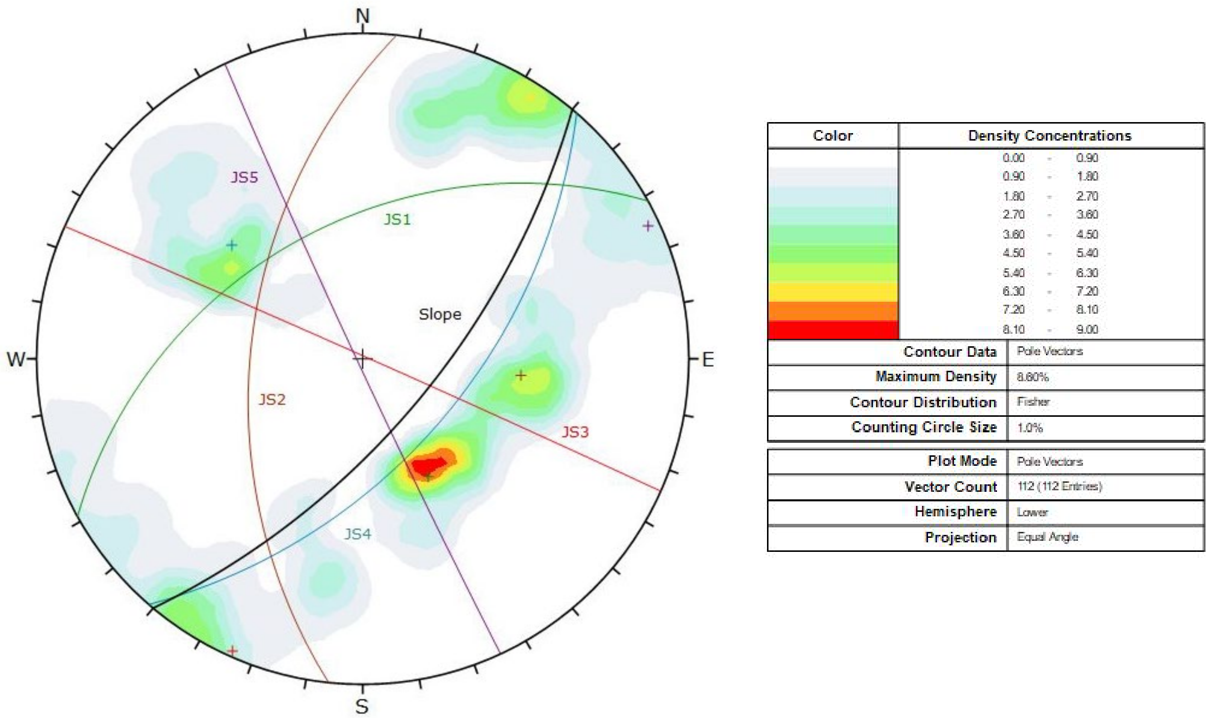

Figure 2.5 Stereonet for Long Lake 75.5 rhyodacite.

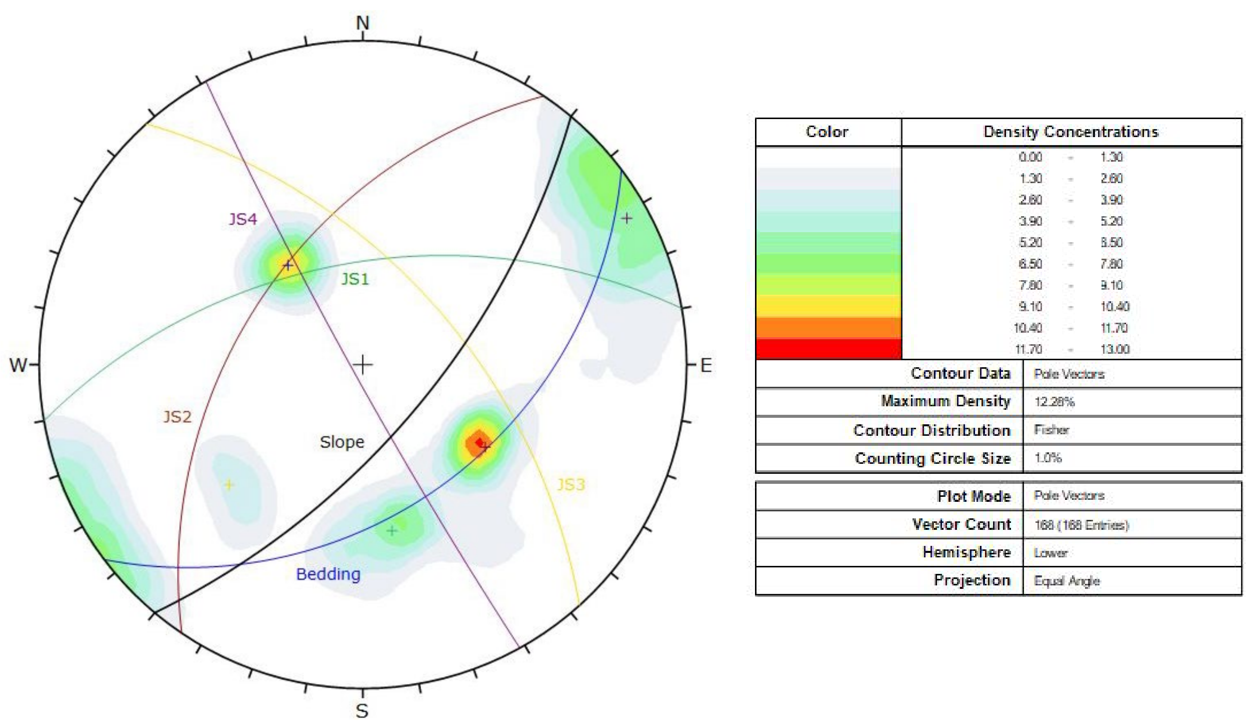

Figure 2.6 Stereonet for Long Lake 75.5 sandstone.

2.2.3. Long Lake MP 85.5

This road cut is 6-m high at a 56° slope, facing 140°. It consists of a gabbro intrusion (Figure 2.7); however, its appearance in the road cut is similar to the nearby sandstone due to jointing. It is part of an Eocene mafic sill, consisting of orthopyroxene, clinopyroxene phenocrysts up to 3 mm, and plagioclase. On June 9, 2021, we performed Schmidt hammer testing at three sites, with both hammer types, and collected samples for point load testing. We also made 94 measurements of joints exposed in the gabbro road cut, which indicate the presence of three main joint sets (Figure 2.8).

Figure 2.7 Road cut in gabbro at LL 85.5 site.

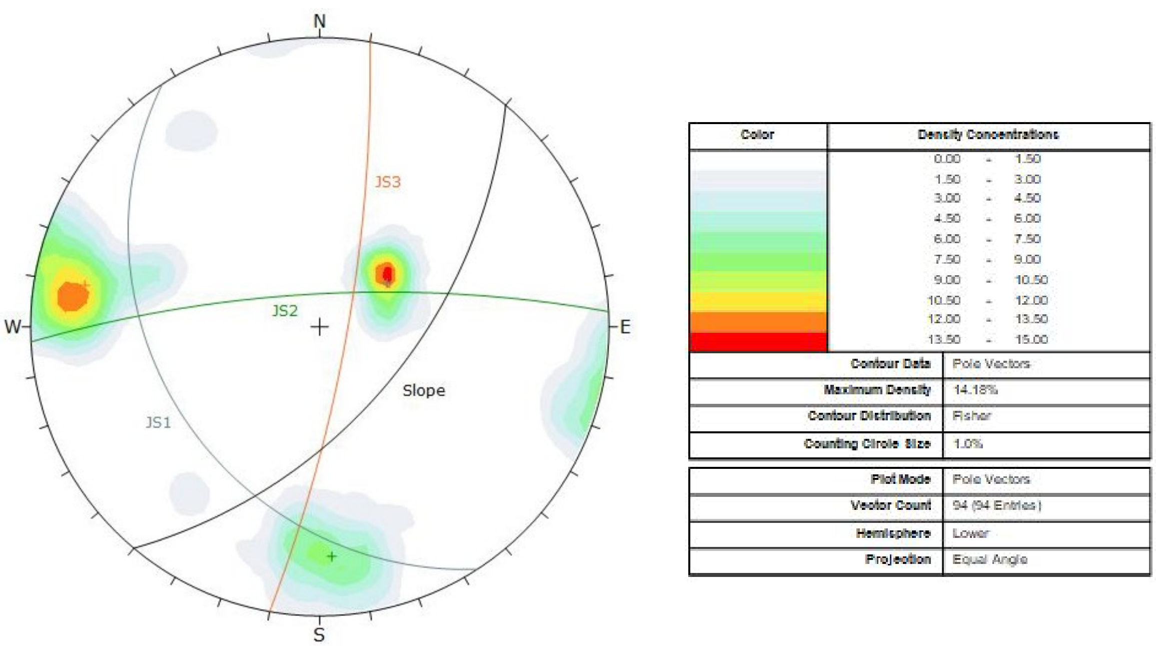

Figure 2.8 Stereonet of Long Lake 85.5 gabbro road cut.

2.2.4. *Long Lake MP 87*

In this area, the Glenn Highway traverses the side of a steep slope, forming a ~760-m long road cut into the Chickaloon Formation (Trop et al. 2015). This road cut is 37-m high at a 60° slope, facing 170°. Above the site, a gabbroic sill forms a prominent cliff, contributing this rock type to the talus and colluvium stratigraphically above the sedimentary bedrock in the area. The road cut consists of interlayered mudstone and poorly-cemented sandstone, with some minor conglomerate as basal layers in the sandstone. Some of these basal layers contain cobbles of carbonaceous mudstone. The lithic sandstone is fine-grained (1/8-1/2 mm), containing quartz, plagioclase, and mica grains, and exhibits cross-bedding. The mudstone is similar to the units present at Long Lake 71 and 75. On June 9, 2021, we performed Schmidt hammer testing at 11 sites with both hammer types, and collected samples for point load testing. For this location, all SH tests were parallel with bedding. We also collected 27 structural measurements. The site demonstrates predominant bedding oriented with dip and dip direction of 42° and 20°, respectively, and a conjugate fault set (Figure 2.9 and Figure 2.10).

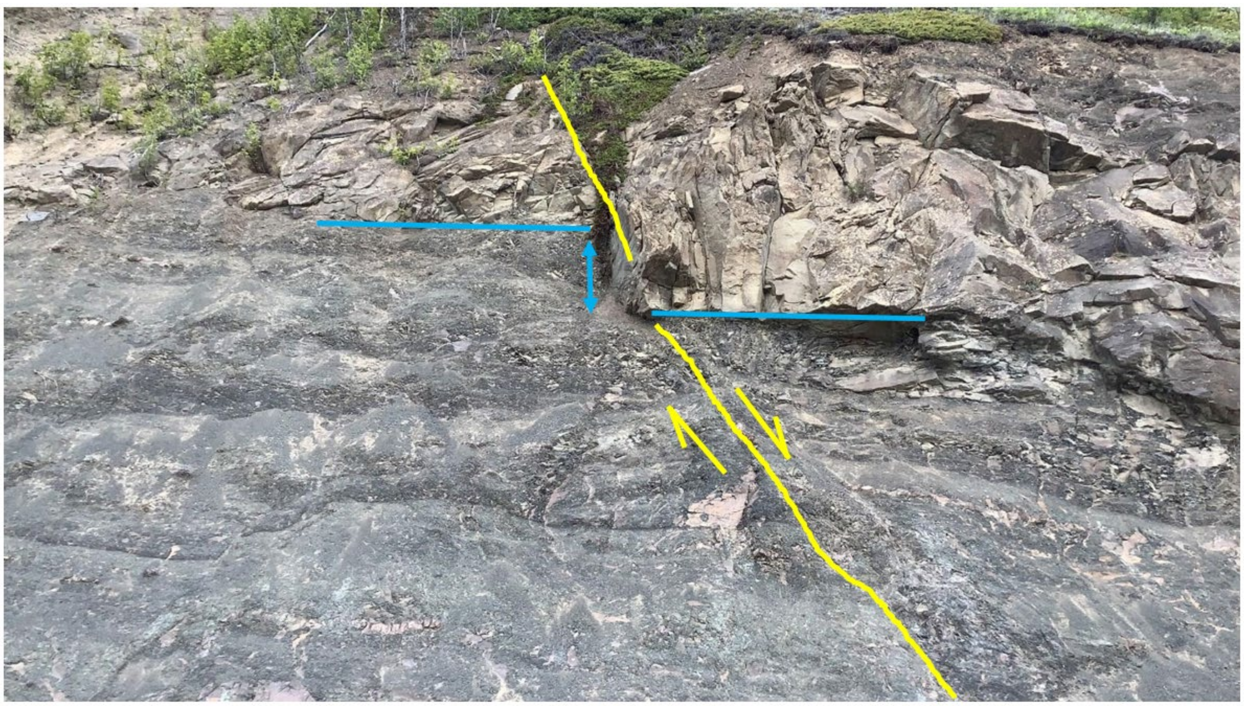

Figure 2.9 Example of a normal fault in the LL 87 area, indicating sense and amount of displacement.

2.2.5. *Long Lake MP 89*

This is a mafic sill exposed as a cliff to the north of the road, and a talus/boulder field at the base of the slope towards the road. The sill is Eocene gabbro (Trop et al. 2015), consisting of orthopyroxene, clinopyroxene (phenocrysts up to 1 cm), plagioclase, and olivine. We conducted one set of Schmidt hammer tests with each instrument on June 8, 2021, and collected two samples for point-load testing.

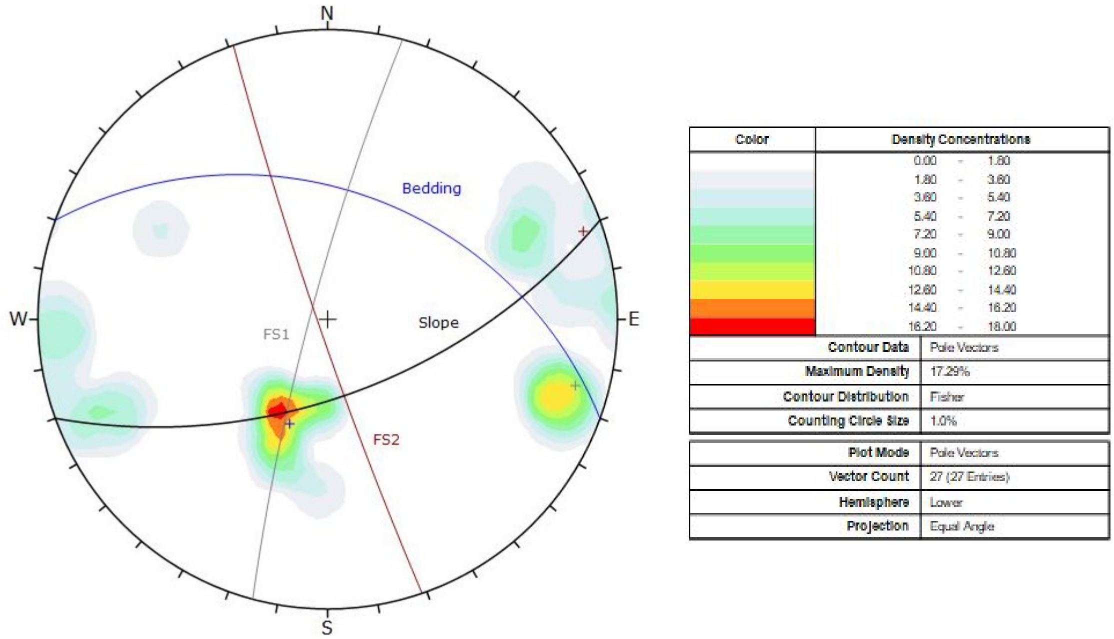

Figure 2.10 Stereonet of Long Lake 87 sedimentary rocks.

2.3. Parks Highway / Nenana Canyon Site Descriptions

The Parks Highway, built in the Nenana Canyon area in 1971, follows the Nenana River through Precambrian to early Paleozoic metamorphic rocks (Csejtey et al. 1986). As evident through hand sample observations, the predominant mineral assemblages suggest continental margin/marine protoliths and greenschist facies metamorphism (Csejtey et al. 1986).

2.3.1. Parks Highway Mile Post (MP) 241

This road cut is ~740-m long, up to 89-m high and at an angle of 80° facing 265°. It cuts through intercalated layers of micaceous quartzite and muscovite/sericite quartz schist. The quartzite is bluish gray and massive in outcrop, and greenish gray in hand sample. The quartzite layers contain pervasive folding including isoclinal folds, crenulations (Figure 2.11), and axial planar cleavage, demonstrating multiple metamorphic events and deformation (Csejtey et al. 1986). Although predominantly quartz, some samples contain minor amounts of calcite and secondary pyrite. The other major rock type is light gray muscovite/sericite quartz schist with minor amounts of calcite (<5%) and chlorite (up to 20% in some samples), which weathers white to red in outcrop.

On June 10, 2021, we performed SH measurements at 14 locations, first with the Type N and Type L, then with a different person performing repeat measurements with the Type N. We collected representative samples for point-load testing, and made 125 structural measurements of discontinuities (cleavage, joints, and faults; see Figure 2.12).

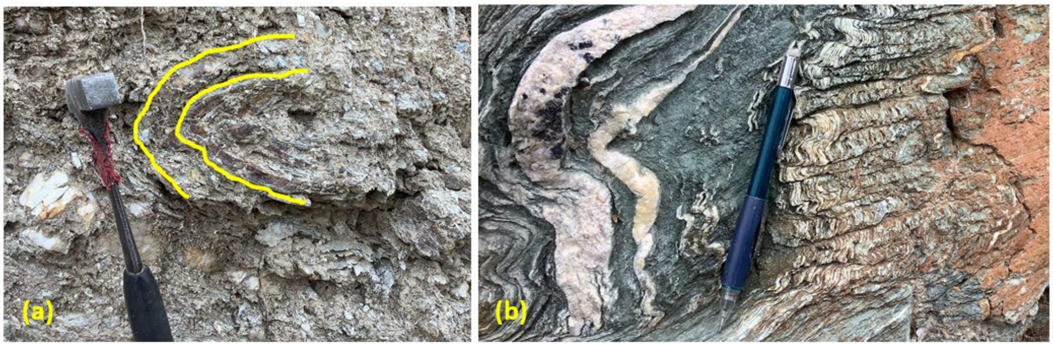

Figure 2.11 Examples of (a) isoclinal (indicated in yellow) and (b) crenulation folds at Parks Highway MP241.

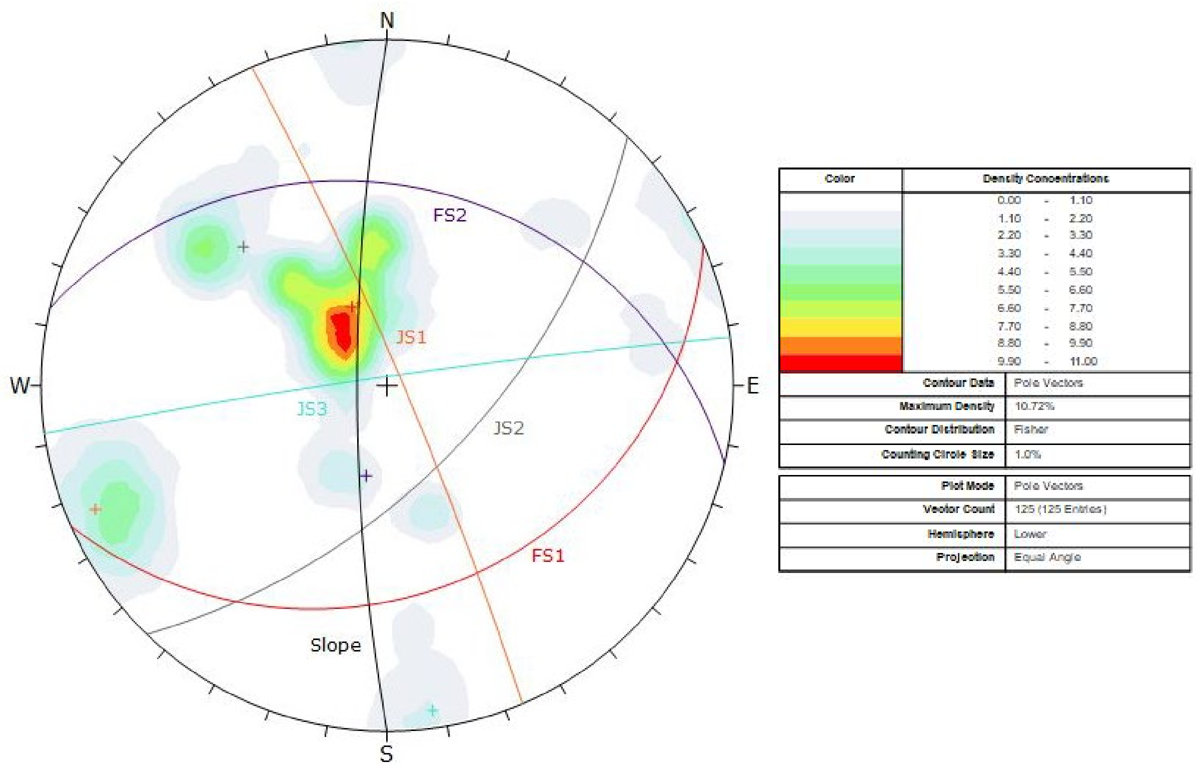

Figure 2.12 Stereonet of Parks Highway MP 241 schist.

2.3.2. Parks Highway MP 239

This ~670-m long road cut (Figure 2.13) exposes both Precambrian to early Paleozoic metamorphic rocks and Tertiary intrusive rocks. The cut faces 230°-270°, is as high as 152 m, and has a general slope of 70°. The metamorphic rocks are intercalated layers of dark gray (bluish-gray in outcrop) micaceous quartzite with up to 20% muscovite, <1% chlorite, and <1% pyrite crystals up to 2 cm; and white to silver muscovite/sericite quartz schist. Although predominantly (~60%) quartz, the schist easily breaks on foliation. At the south end of the road cut, there is a small area of dark gray quartz muscovite schist (20% quartz, 80% muscovite), and to the north of the road cut, is massive, non-foliated quartzite with 2-5% biotite and <1% pyrite. This exposure of quartzite is extremely strong rock based on field tests (Wyllie and Mah 2004). Along the road cut in several locations are exposures of dark gray to black

Figure 2.13 Recent rockfall behind barrier along the Parks Highway MP239 rock slope.

diabase dikes that intruded the schist. The diabase contains plagioclase feldspar (up to 0.5 mm) and hornblende, with some magnetite.

On June 11 and 12, 2021, we performed SH measurements at 18 sites. At two sites, we tested both perpendicular to and parallel with the foliation. We tested a concrete barrier to check similarities among readings and between the Type N and Type L hammers. We also performed grid measurements, where we set up a grid of points, spaced 20 cm apart, with 16 points into the foliation (the predominant direction for all other sites), and six points perpendicular to foliation. First Type L measurements were made, followed by Type N. We also collected representative samples for point-load testing, and made 184 structural measurements of joints in the basalt, and 196 structural measurements of cleavage, joints, and faults in the schist. Figure 2.14 and Figure 2.15 are stereonets of the structural data for the diabase and schist, respectively.

2.4. Results of Rock Strength Field Tests

Although we collected point-load tests from both years of field tests, the results from 2021 were erroneously low. We attribute this to leakage of hydraulic fluid from the device while in the field, and thus do not include those results here. We had a similar equipment issue with the L-type Schmidt hammer that we used in 2021. Based on the low values obtained, we suspect that the hammer requires

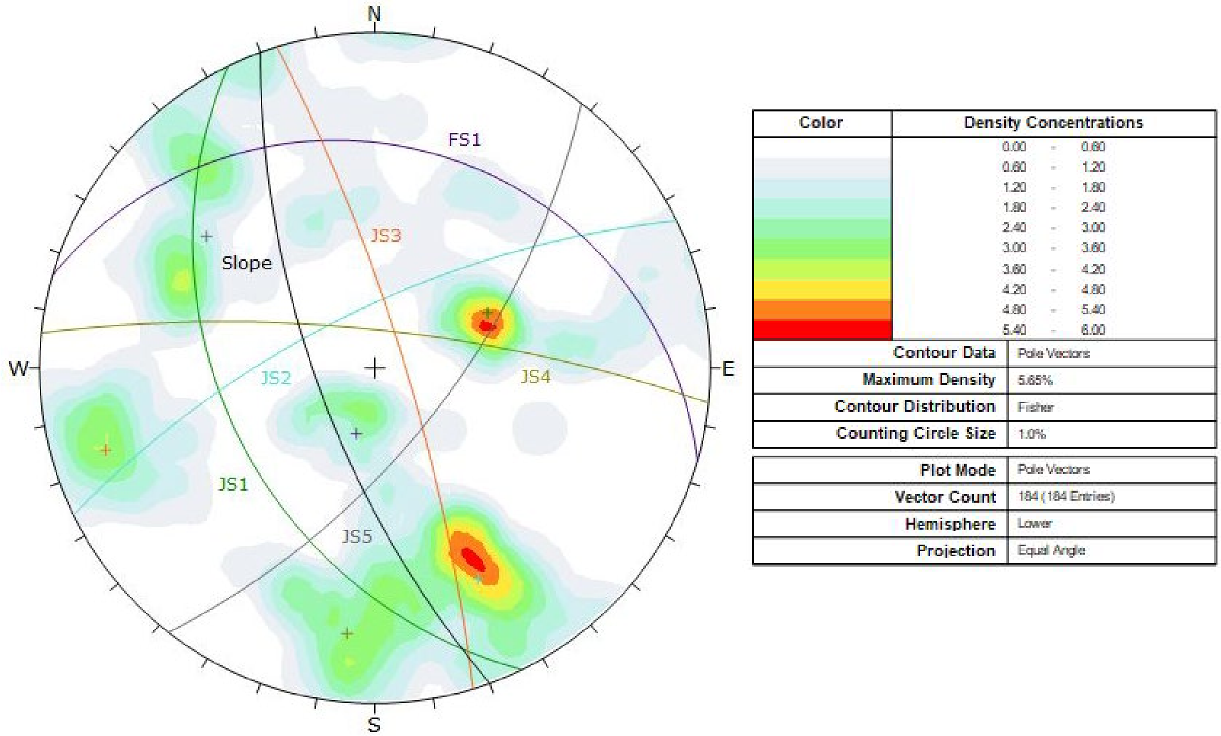

Figure 2.14 Stereonet of Parks Highway MP 239 diabase exposure.

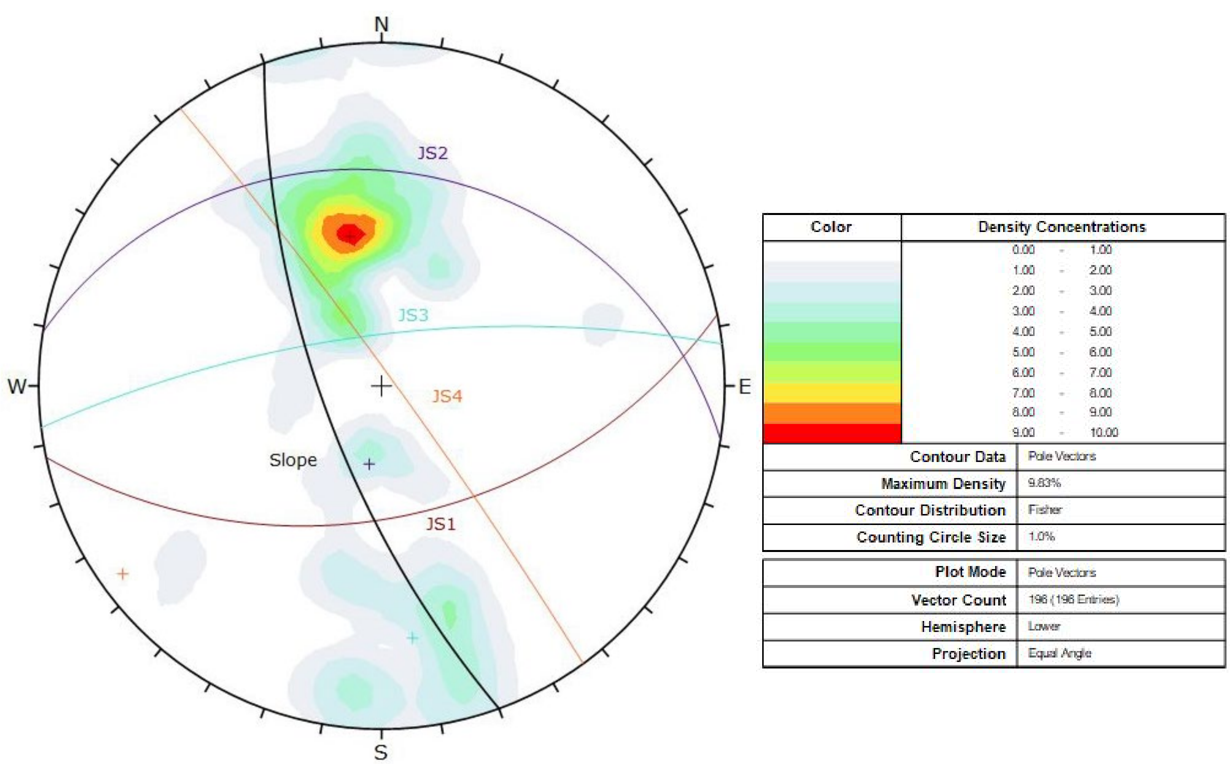

Figure 2.15 Stereonet of Parks Highway MP 239 schist.

calibration. Thus, Table 2.1 is a summary of limited results obtained from the point-load tests and Schmidt hammer readings collected in the field. Each value represents the average of all tests conducted during the respective year. Comparison of the field results to published uniaxial compressive strength values (Table 2.1) indicates that the results for sedimentary rocks fall within published limits, whereas results for the igneous and metamorphic rocks are lower than published values. Because of the equipment issues, we consider these values as preliminary, and as part of future work, we will conduct a systematic field-testing program with calibrated Schmidt hammers and compare those results to laboratory tests of uniaxial compressive strength of collected rock samples.

Table 2.1 Summary of field-test results of rock strength. Number of tests are indicated in parentheses. '*' data from Attewell and Farmer (1976).

Location	Rock type	Avg strength (MPa)			Published uniaxial compressive strength values (MPa)*
		2020 point-load test results	2021 N-type Schmidt hammer		
			Results	Std dev.	
Long Lake 71	Mudstone	27.9 (4)	26.1 (11)	10.8	5-100 (shale)
Long Lake75	Rhyodacite	87.3 (2)	118.7 (3)	56.5	---
	Sandstone	97.9 (2)	70.7 (2)	---	20-170
	Mudstone	40.2 (2)	---	---	5-100 (shale)
Long Lake 85.5	Gabbro	---	43.2 (3)	17.3	150-300
Long Lake 87	Sandstone	17.5 (3)	41.9 (9)	11.1	20-170
	Mudstone	---	20.9 (2)	---	5-100 (shale)
Parks Hwy 241	Schist	25.1 (3)	34.9 (24)	20.9	---
	Quartzite	---	33.3 (4)	11.9	150-300
Parks Hwy 239	Diabase	95.2 (2)	88.4 (6)	35.3	100-350
	Schist	36.4 (1)	41.2 (30)	15.5	---
	Quartzite	---	82.7 (2)	---	150-300

CHAPTER 3. INFLUENCE OF 2018 ANCHORAGE EARTHQUAKE ON PERSISTENCE OF ROCKFALL ACTIVITY AT LONG LAKE MILEPOST 71

Following the November 30, 2018 $M_w7.1$ Anchorage earthquake, there were multiple reports of lateral spreads, liquefaction, landslides, and rockfall in proximity to the area of rupture (West et al. 2020). One of the rock slope sites that has been subject to characterization and repeat laser scanning as a part of PacTrans work – Long Lake Milepost 71 (LL71) – was within the range of shaking, and according to US Geological Survey shakemaps, was subject to accelerations of 0.08-0.12g. While modest in terms of acceleration magnitude, the significant aseismic activity at this site served as a prime opportunity for strategic data collection to constrain (1) coseismic rockfalls, and (2) the timing and magnitude of post-seismic rockfall activity from an active rock slope. Thus, we collected several terrestrial lidar scanning (TLS) datasets through an NSF RAPID grant over the following year, and thereafter we continued to monitor medium- to long-term rockfall activity at LL71 through this effort.

Since 2012, we have collected terrestrial lidar (TLS) at LL71 on approximately a yearly basis, with the exception being a two-year gap starting in 2015 and more frequent data collection (as short as 29 days between TLS collects) following the 2018 Anchorage earthquake. Table 3.1 is a summary of the lidar collection epochs at the site. Earthquakes are known to drive rockfalls, but their lingering effects on rockfall activity are poorly-constrained. We used change analysis of digital terrain models (DTMs) to evaluate the persistence of rockfall following the 2018 earthquake. Change was determined through differencing DTMs that were spatially rectified to best-fit planes and processed to remove vegetation and artifacts. Through subtraction of DTM grids (resolution of 0.05 m, significant change of 0.02 m), we evaluated change as a function of rockfall clusters. We created a script using connected components to evaluate clusters of change between epochs (and exceeded the significant change threshold) to evaluate the volume of individual rockfall clusters. We recorded over 220,000 rockfalls over the ten-year period since the start of data collection, over 144,000 of which have occurred since the earthquake. Of course, some of this may owe to a bias in data collection frequency since shaking; however, even on a *per annum* basis, rockfall frequency remains higher (~70 rockfalls/day) versus the pre-seismic rates (~45-60 rockfalls/day).

Table 3.1 TLS Collections for LL71

Data Collection Date	Epoch Length	Rockfalls	Rockfalls/Day
August 5, 2013	---	---	---
July 28, 2014	357	21,297	59.6
August 25, 2015	393	22,277	56.6
August 14, 2017	720	15,097	20.9
September 2, 2018	384	17,954	46.7
November 30, 2018	----- ***EARTHQUAKE*** -----		
April 9, 2019	219	34,045	155.4
May 9, 2019	30	18,940	631.3
June 4, 2019	26	20,484	787.8
August 15, 2019	72	18,157	252.1
September 1, 2020	383	25,498	66.5
June 8, 2021	280	27,440	98.0

A more telling behavior is cumulative rockfall volume (m^3) and rockfall rates (m^3/day) over the span of monitoring LL71. As shown in Figure 3.1, cumulative rockfall volume and rockfall rates are variable over the timeframe of monitoring. The raw data (Figure 3.1a, c, and e) demonstrate an uptick in rockfall volume and rate prior to the earthquake, owing to a single rockfall of approximately 87 m^3, which is in fact the largest rockfall observed during the entire monitoring period. As events of this magnitude are infrequent and stochastic, we may consider this event an outlier and look at rockfall rates considering smaller, more frequent (and thus potentially more hazardous) rockfalls. There is a steepened slope in cumulative rockfall volume following the earthquake, both from coseismic and post-seismic rockfall activity (Figure 3.1b, d, and f). This is further reflected in rockfall rates, which are heightened following the earthquake. While the large spike likely owes to a spike in released rockfall volume during a warm spring and short TLS collection intervals, the overall, approximately-yearly intervals still indicate rockfall rates being approximately 80%, 40%, and 10% greater than mean pre-seismic rates in 2019, 2020, and 2021, respectively. While this is a moderately-rapid return to baseline rockfall activity, this suggests that even relatively modest seismic disturbance can result in a period of heightened rockfall hazard. Moreover, it demonstrates that following an earthquake, transportation planners may consider a period where increased maintenance is employed or further warning is provided to motorists near active, hazardous rock slopes. Of important note is that the coseismic and post-seismic rockfall rates do not owe to anomalous climatic forcing – that is, the cumulative rainfall generally follows seasonal normal (Figure 3.2), whereas departure of cumulative precipitation and snow-water equivalent were within 5% of typical conditions in 2019, 2020, and 2021.

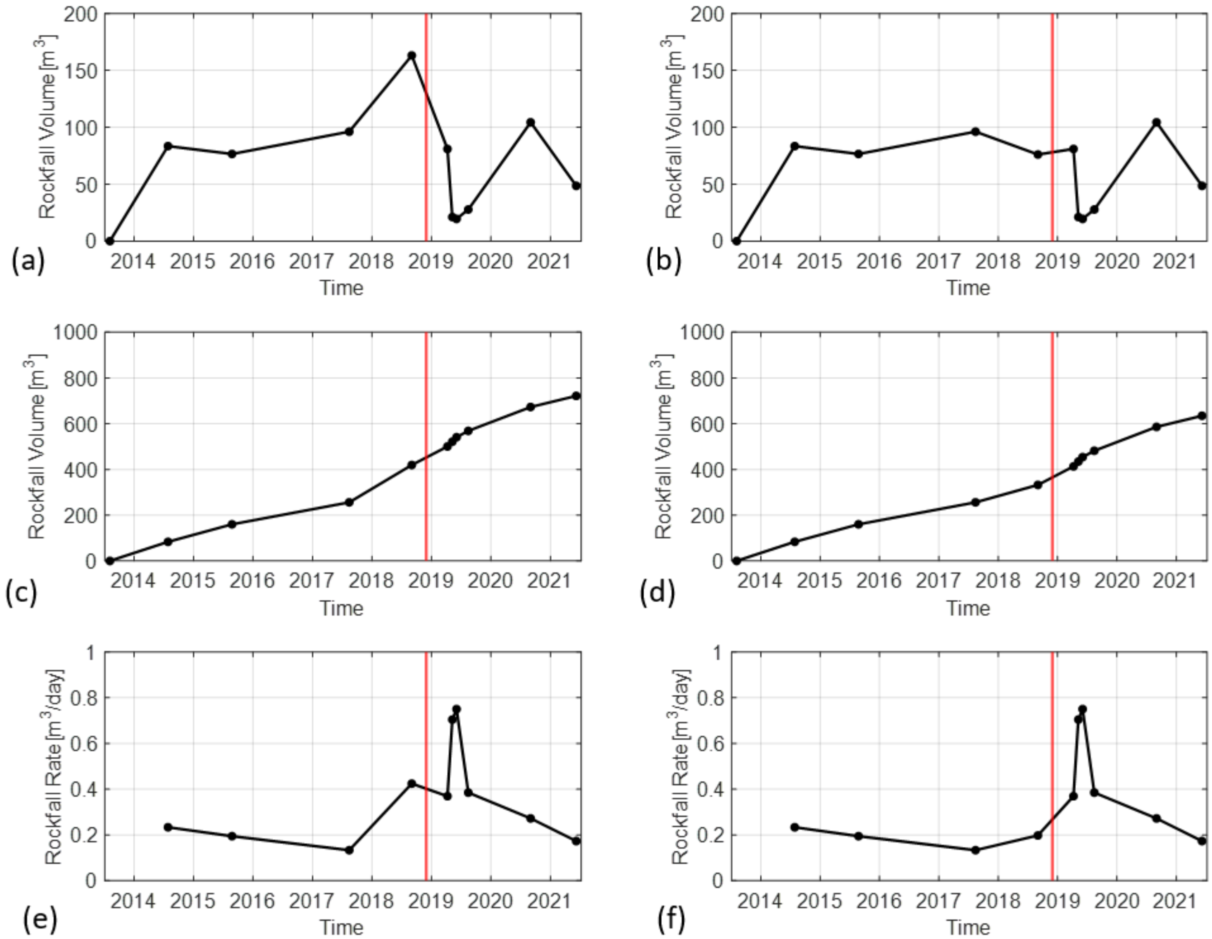

Figure 3.1 Rockfall results for LL71. Sub-figures (a), (c), and (e) display rock slope behavior including all rockfalls, whereas sub-figures (b), (d), and (f) display rock slope behavior excluding the largest rockfall event that occurred prior to the earthquake (~87 m^3 between 2017 and 2018 TLS collections). Sub-figures (a) and (b) are the volume of rockfalls in each epoch, (c) and (d) are cumulative rockfall volume over the span of monitoring, and (e) and (f) are normalized rockfall rates over the span of monitoring. The red vertical line represents the date of the 2018 Anchorage earthquake.

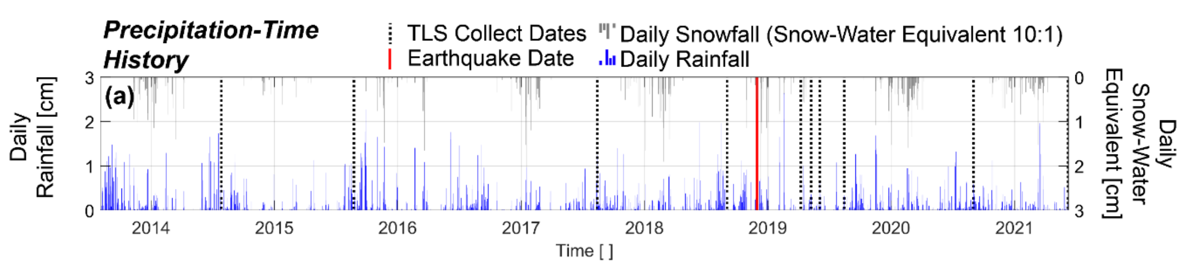

Figure 3.2 Climate activity at LL71 over the monitoring period, averaged from the three closest weather stations: Lazy Mountain (COOP 505464-5), East Palmer (SNOTEL 953), and Palmer (AFC).

CHAPTER 4. REGIONAL SEISMIC ANALYSIS

4.1. Rockfall Activity Rate System

The Rockfall Activity Rate System (RoARS; Massey et al. 2022) predicts the volume of rock that is likely to fall from a slope during a seismic event based on the slope's geometry, the increase of non-earthquake rockfall rates after a seismic event, and the amount of time until post-earthquake rockfall rates decrease to pre-earthquake rates. The RoARS calculations consist of four principal steps as described in Massey et al. (2022):

1. Using a given rock slope and a given earthquake scenario, the first step is to predict the potential rockfall volume from the rock slope under the defined seismic event.
2. Next, the rockfall rates of the rock slope prior to the seismic event (pre-earthquake rockfall rates) are determined.
3. The third step is to estimate the increased rate of rockfall on day one of the earthquake (non-earthquake increases in rockfall rates). This step is accomplished by first estimating a factor of increase of the earthquake rockfall rates above the pre-earthquake rates and then estimating the post-earthquake factor of increase in the non-earthquake rates above the pre-earthquake rates.
4. Finally, the time after the earthquake occurs for the rockfall rates to decrease from the non-earthquake rockfall rates to the pre-earthquake rates is determined.

While RoARS was developed based on the response of rock slopes in New Zealand to seismic activity, the methodology can be applied to our Alaskan study sites to show the general risk of each rock slope given seismic activity. The study sites used also have well-documented rockfall history from repeat TLS scans; hence should the results of applying RoARS prove to be unrealistic, we can determine how to adjust the RoARS methodology to make it more applicable.

4.1.1. Computed earthquake-induced rockfall volumes

STEP 1: We determined the earthquake-induced rockfall volumes using an empirical relationship between the volumes of rockfall and the earthquake PGA that was established from the Port Hills rock slopes after the Canterbury New Zealand Earthquake Sequence (CES) (Olsen et al. 2020; Massey et al. 2022). These volumes were determined by comparing the differences between terrestrial and airborne lidar surveys before and after the main CES earthquakes. Next, we calculated a rate by dividing the volume eroded by the product of the area of the slope and the time between surveys (Eqn 4.1):

$$R = \frac{Vol}{A*t} \qquad \text{Eqn 4.1}$$

where *R* is rate, *Vol* is the volume, *A* is the surface area of the slope, and *t* is the time between surveys. Some surveys did not have earthquakes happen between them; hence, we referred to the estimated rockfall rates calculated from them as "non-earthquake" rockfall rates. "Earthquake" rockfall rates were determined using surveys that had a major earthquake happen between them and the volume of rockfall was assumed to be a response to the earthquake. Using the lidar scans, we determined specific parameters such as maximum slope height (from slope toe to crest), mean slope angle, and surface area. For one rock slope, the slope height and angle were kept constant between scans, but the slope angle and volume were different depending on the "epoch." For more details on the specific rock slopes studied and the volume estimation models, please refer to Olsen et al. (2020). From the rock slope observations at the CES study site, an empirical forecast model was created to predict the total rockfall volume that could be produced from a rock slope during an earthquake. The variables considered were slope height, slope angle, slope area, and horizontal PGA. The regression models we considered were a multiple linear "least squares" regression, a multiple polynomial regression, and a multiple log-linear regression (i.e., power-law). The log-linear, power-law model provided the best fit to the data (Eqn 4.2) and the most significant variables were slope height, slope angle, and PGA (listed in order of significance). More information on the rock slopes tested to derive this relationship can be found in Massey et al. (2022). The resulting equation is:

$$logVol_{EQ(t1)} = 6.431 \times log\alpha_{ave} + 1.6576 \times logH_{max} + 0.526 \times logPGA_H - 37.122 \qquad \text{Eqn 4.2}$$

where $logVol_{EQ(t1)}$ is the logarithm of the post-earthquake rockfall rates that are computed as the volume of the material normalized by slope area in m^3/m^2 resulting from the earthquake event with the given PGA_H; $log\alpha_{ave}$ is the logarithm of the average slope angle (°), $logH_{max}$ is the logarithm of the maximum height of the rock slope portion of the slope (m), and $logPGA_H$ is the logarithm of the forecast horizontal free-field PGA for rock conditions (m/s^2).

STEP 2: Next, baseline, non-earthquake rockfall rates need to be determined. These can be determined from repeat terrestrial lidar surveys over several years to account for variability in climate. Massey et al. (2022) determined pre-CES rockfall rates using estimations found in the Litchfield et al. (2016) and Massey et al. (2015) studies. Litchfield et al. (2016) found that the age of the debris/rockfall deposits at the study slopes were younger than 1,300 years BP and consisted of 50% beach sand. Massey et al. (2015) estimated the deposit volumes, and determined the pre-CES rockfall rates by dividing the estimated volumes in half – to account for the volume of beach sand and potential bulking of talus – and then by 1,300 years to find the average deposit volume per year. These rockfall rates were assumed to be constant over time based on an average value over a long time period. These rates were more likely event driven and not constant over time; more information about the study slopes can be found in Olsen et al. (2020).

STEP 3: First, we estimated the increase in non-earthquake rockfall rates by dividing the volume of rockfall in response to the first major earthquake by the mean and upper estimates of the pre-CES debris accumulation rates estimated for each site. The factor of increase in non-earthquake rockfall rates above the pre-CES rates on day one after the 22 February 2011 earthquake was estimated by dividing the volume of debris that fell from the cliffs from each difference-model epoch (i.e., for those epochs where no major (>0.4 $\mathrm{m/s^2}$ PGA) earthquake occurred) by the time after the 22 February 2011 earthquake. We defined a major earthquake as one that produced a PGA > 0.4 m/s^2. This is based off a mid-range of coseismic landslide thresholds presented by Jibson and Harp (2016); similar ground shaking intensities are suggested by others (e.g., Del Gaudio and Wasowski 2004, Wilson and Keefer 1985). Using a power law trend for the data for each site, we extrapolated the rockfall rates on day one after the 22 February 2011 earthquake. The relationship between the factor of increase of the non-earthquake rockfall rate on day one after the 22 February 2011 earthquake above the pre-CES rate and the factor of increase of the rockfall rate caused by the 22 February 2011 earthquake above the pre-CES rate can be seen in further detail in Olsen et al. (2020).

STEP 4: We estimated the post-earthquake decay in rockfall rates by plotting the factor of increase in the non-earthquake rockfall rates above the mean and upper pre-CES rates over time. We determined the mean and upper estimates for the time expected for the rock slope to return from non-earthquake rockfall rates to pre-CES rates using a power law trendline. Further details about this process can be found in Olsen et al. (2020) and Massey et al. (2022).

4.2. Data Preparation

Olsen et al. (2020) created a computation spreadsheet to calculate the ROARS estimates. In order to apply the RoARS methodology to the Alaskan study sites in a batch process, we created two ArcGIS Pro tools (Figure 4.1). The appendix contains the Python scripts for each tool (from Holtan 2021). The first GIS tool extracts the necessary parameters for calculations and is called “01_Parameter Extraction,” and the second tool – called “02_ROARS Analysis” – computes the RoARS calculations.

4.2.1. Data Compilation

Building on the RIM database from a prior PacTrans project, we used rock slope inventory data from the Alaska Department of Transportation and Public Facilities (ADOT&PF) Geotechnical Asset Management (GAM) program for the analysis.

4.2.2. ADOT&PF GAM Program: Rock slopes

The ADOT&PF has been expanding their GAM program over the last decade to document rock slopes, unstable slopes and embankments, retaining walls, and materials sites owned by the ADOT&PF (Figure 4.2). The program’s primary focus is on characteristics that can deteriorate over time and creating

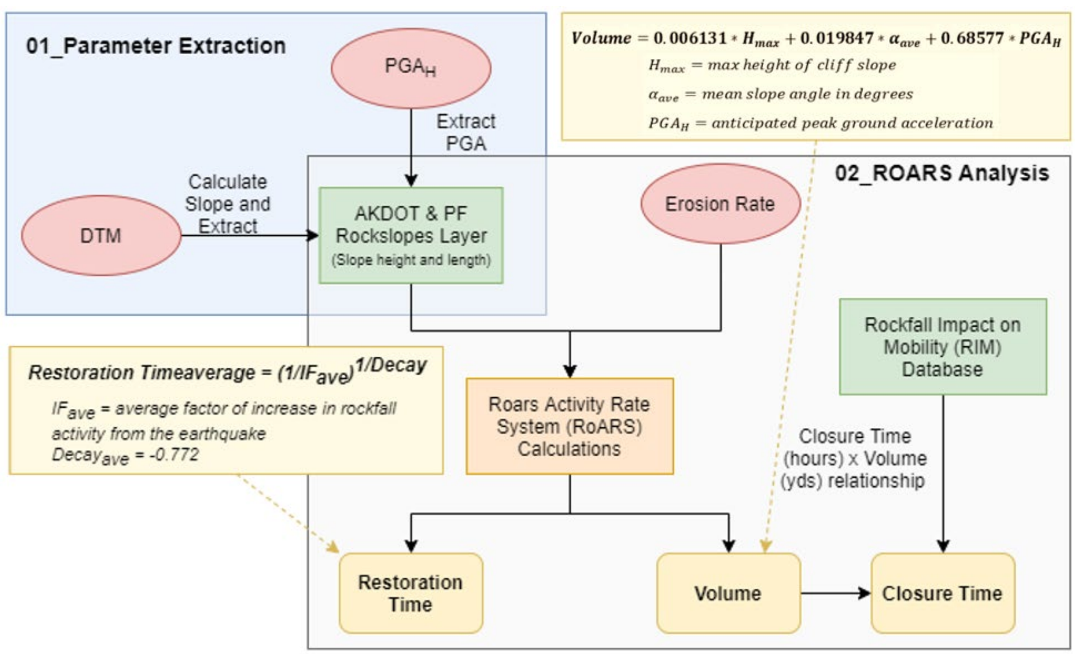

Figure 4.1 RoARS methodology for application and associated tools.

deterioration models that can determine the life-cycle cost and return on investment. The ADOT&PF GAM database contains detailed information for rockfall-prone slopes including rockfall hazard rating system scores, Average Annual Daily Traffic (AADT), speed limit, roadway width, sight distance, resources applied (e.g., maintenance), and accident information. It also includes basic slope geometry information such as the length and height as well as the failure type (rock avalanche, block, planar, raveling/undermining, toppling, and wedge). This information is then aggregated into a condition index, condition state, and estimated improvement cost. This database is available in a webGIS format that is searchable and straightforward to analyze (Figure 4.3). Similar to the Oregon Department of Transportation (ODOT) Unstable Slopes database, the number of yearly rockfall events is highly variable, predominately from potential variability in reporting or localized climatic events that result in clusters of rockfalls (Figure 4.4). Nonetheless, many unstable rock slopes show repeat rockfall events (Figure 4.5). This supports the need to track and catalog rockfall events as a means of prioritizing planning resources to increase the cost-effectiveness of mitigation efforts.

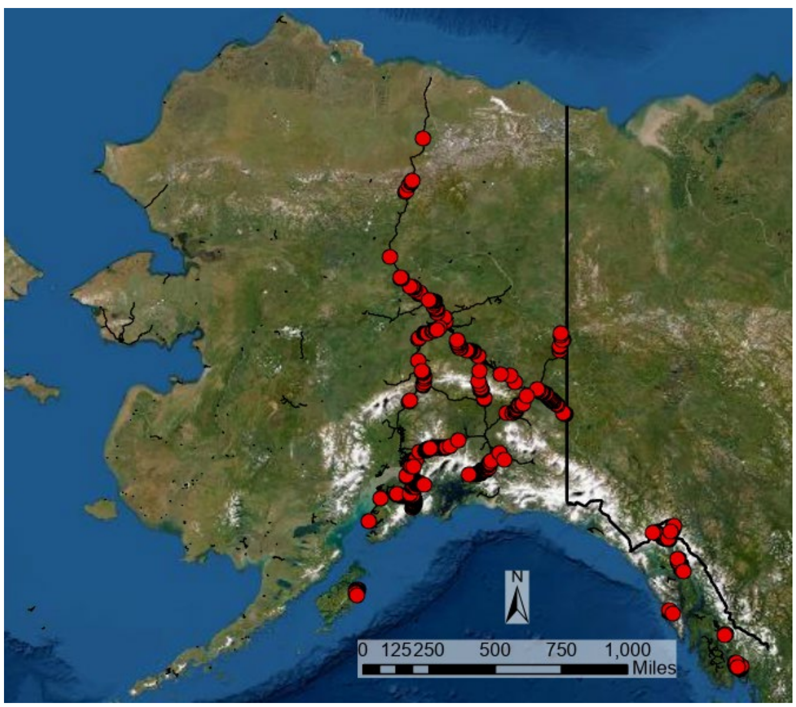

Figure 4.2 Map of the ADOT&PF rock slopes and other features tracked in GAM (road data from the ADOT&PF 2020).

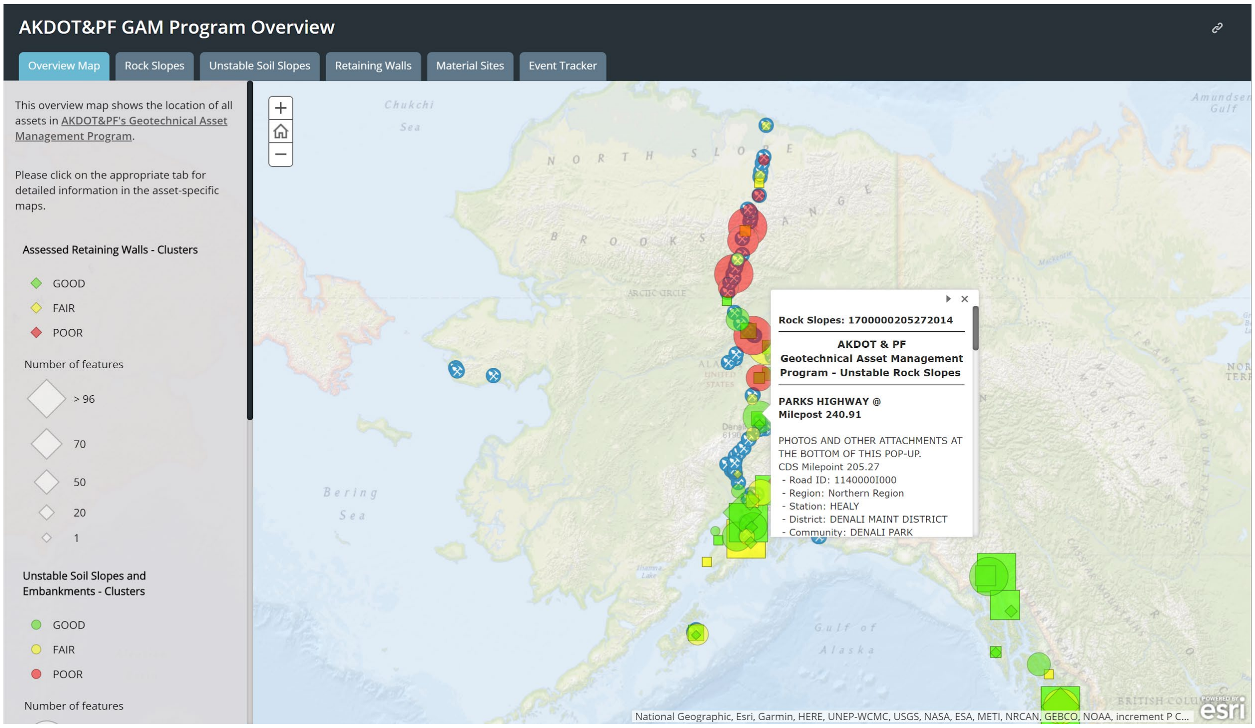

Figure 4.3 Example of the ADOT&PF GAM database web viewer.

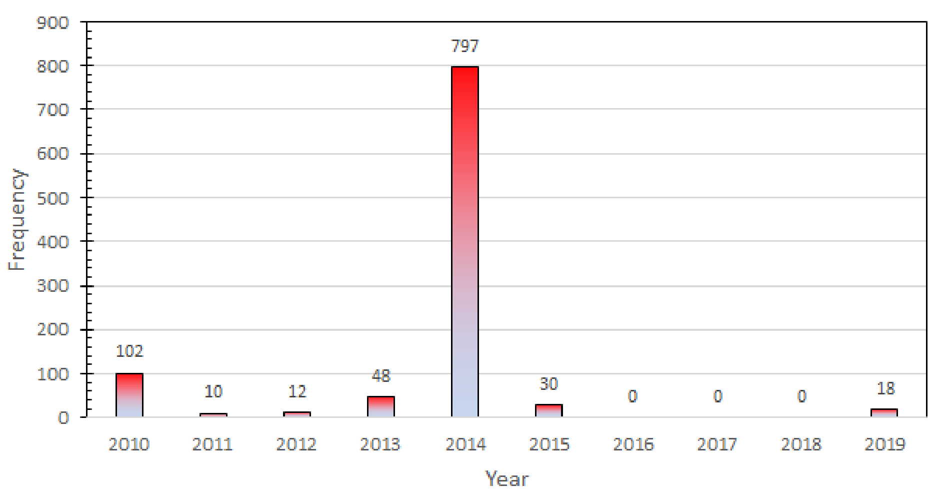

Figure 4.4 ADOT&PF rock slopes event frequency per year.

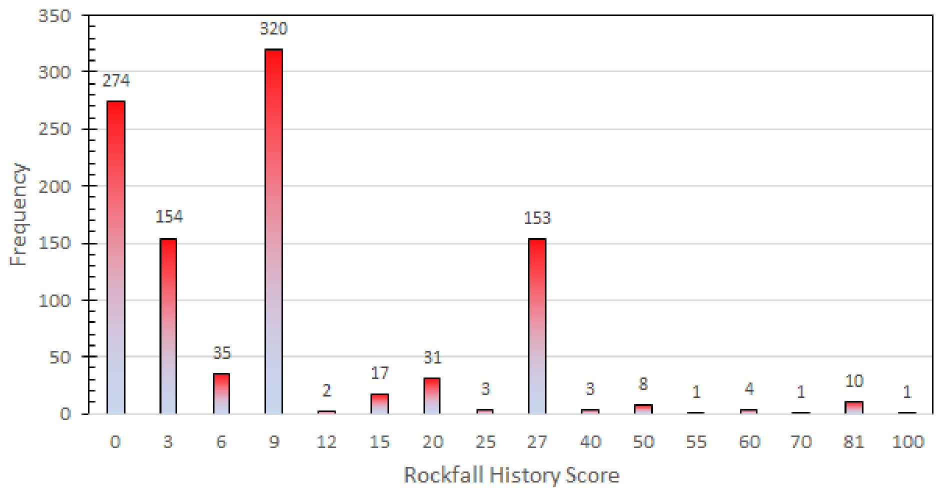

Figure 4.5 Comparison of ADOT&PF rock slopes frequency and rockfall history score.

4.2.3. ADOT&PF Geo-Event Tracker

The ADOT&PF Event Tracker (Figure 4.6) is part of the ADOT&PF GAM program, which tracks events based on maintenance logs. It displays both clustered events and individual incidents containing fields including event type, date, closure duration, resources applied, accidents, event size, cost, and roadway details (Figure 4.7). These attributes are estimations with closure containing ranges of time (less than an hour, between 1-6 hours, between 1 week and 1 month, etc.) and size being described as routine-minor, moderate, major, or catastrophic. The high-quality tracking indicates that rockfalls are a perennial issue in Alaska (Figure 4.8), but still variable with time as shown in other databases. Table 4.1 is a summary of the attribute codes for event type, closure duration, event size, as well as counts of records corresponding to each code.

4.2.1. Tool 1: Data Extraction

The first tool requires seven inputs (Table 4.2): Rockslopes Point Feature Layer, Centerlines Line Layer, Output GDB, Label, DTM, PGA Raster, and Phase. The first input, the Rockslopes Point Layer, is a point layer with points in the area of interest (AOI) located on the rock slopes near roadways, as well as fields for their slope height and slope length. The Centerlines Layer contains a single polyline feature representing the road centerlines in the AOI. The DTM raster contains the elevation in the AOI, while the PGA raster contains spatially-computed PGA estimates for the specific seismic event to be studied. For both rasters, higher resolution is preferred. The first script is run in two phases in order to reduce computation time. The specific phase can be chosen with the final parameter ("Phase") and none of the inputs need to be changed between runs.

The primary objective of this tool is to extract the slope angle and PGA for each rock slope. The Rockslopes Point Layer used in this study is the ADOT&PF RockSlopes layer, which does not contain either the slope angle or PGA estimate for each rock slope; however, if a different rock slope layer is used that already has slope values from field investigations and PGA values already extracted, the first tool can be skipped as long as the slope angle and PGA field are named "*Max_Slope*" and "*PGA,*"

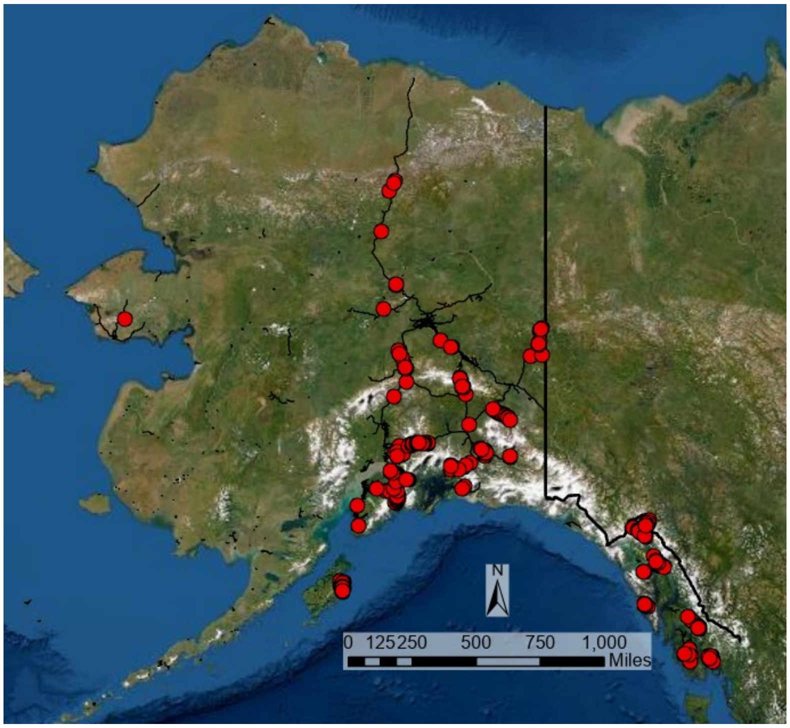

Figure 4.6 Map of the ADOT&PF Geo-Event Tracker (road data from the ADOT&PF 2020).

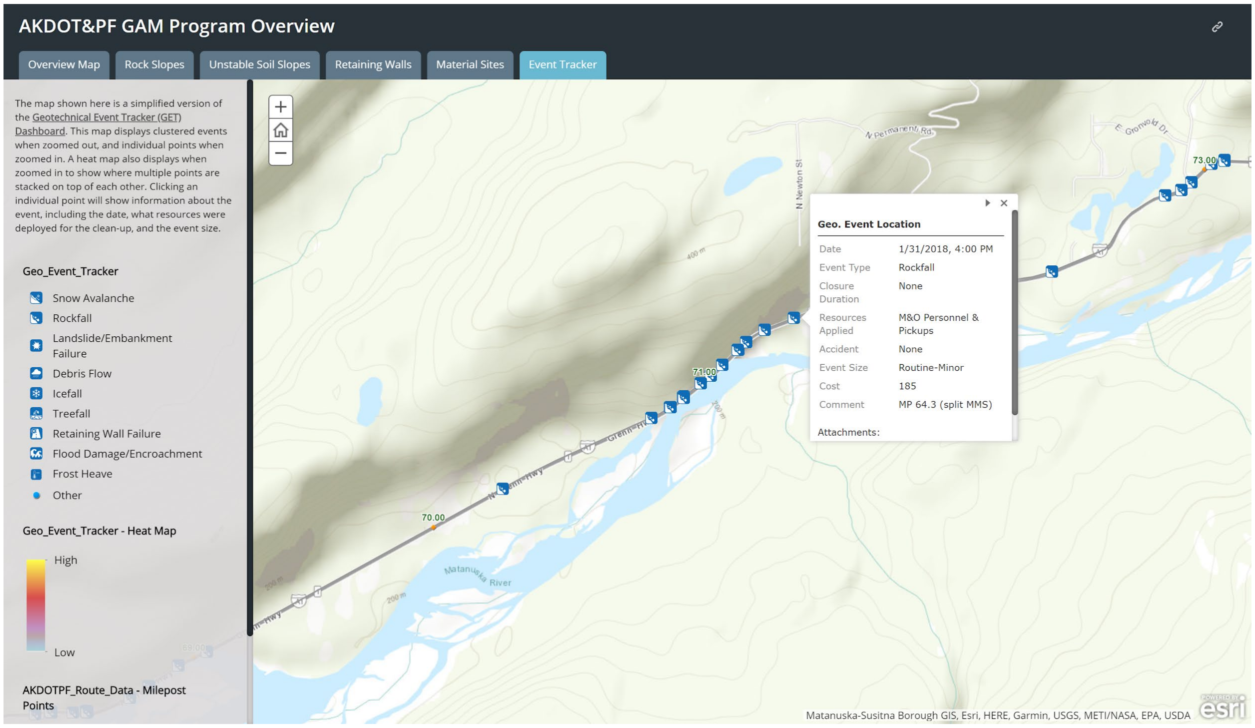

Figure 4.7 Example of the ADOT&PF GAM data viewer with data for a particular event.

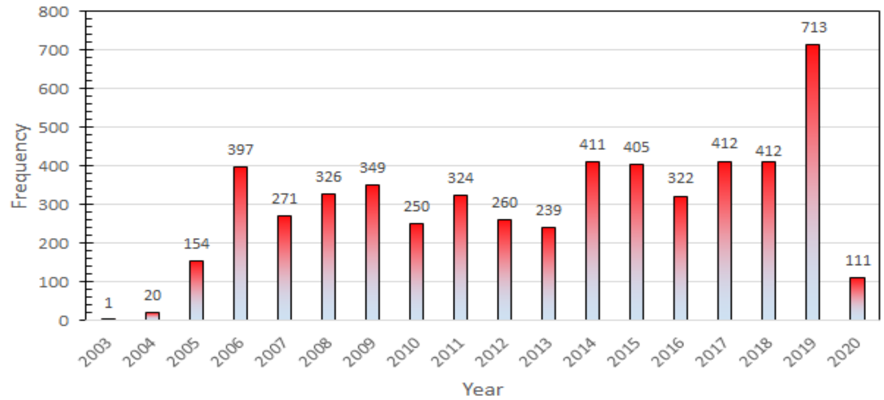

Figure 4.8 Rockfall frequency by year in Alaska.

Table 4.1 Event type in ADOT&PF GAM database

Code	Event Type	Count	Closure	Count	Size	Count
0	Rockfall	4,549	None	11,160	Routine – Minor	7,070
1	Landslide / Embankment Failure	827	Temp. Slow. < 30 min	11	Moderate	2,188
2	Debris Flow	374	Temp. Slow. 30 min – 2 hrs	13	Major	1,380
3	Frost Heave	0	Temp. Slow. > 2 hr	11	Catastrophic	599
4	Snow Avalanche	5,479	Closure < 1 hr	4	---	---
5	Icefall	2	Closure 1 – 6 hrs	25	---	---
6	Retaining Wall Failure	1	Closure 6 – 24 hrs	7	---	---
7	Treefall	2	Closure 24 – 72 hrs	5	---	---
8	Flood Damage	0	Closure 72 hrs – 1 wk	1	---	---
9	Other	3	Closure 1 wk – 1 mo	0	---	---
10	---	---	Closure > 1 mo	1	---	---

respectively. One of the benefits of this tool is that the location of the RockSlopes points do not need to be at the exact location of the top of a given rock slope. The *Max_Slope* values are extracted by first creating perpendicular lines from the points to the centerlines. Then, a buffer is used from the centerlines to extend the perpendicular lines. The perpendicular lines and buffer are combined into one merged layer (Figure 4.9), and the maximum slope along the perpendicular line for each point is extracted. The *PGA* is extracted at the location of the rock slope provided in the initial rock slopes layer. This parameter is less sensitive to a precise location given that it does not vary substantially over a large area. Ideally, it would be close to the centroid of the rock slope.

Table 4.2 Description of Input Parameters in the Tool "01_Parameter Extraction"

Input Field	Data Type	Description	Notes/Assumptions
Rockslopes Point Layer	Point Layer	Point layer that contains the slope height and length of each rock slope and where the points are roughly located on the slope	1. Slope Height Field Name = MSHeightN 2. Slope Length Field Name = MSLengtN
Centerlines	Line Layer	Road centerline layer for the AOI	Only one centerline feature (merge line features prior to running)
Output Geodatabase (GDB)	Workspace	Output geodatabase to store the new feature classes	Assumed GDB
Label	String	Input becomes the prefix to all the output files for easy identification	Can contain letters and/or numbers
DTM	Raster Layer	DTM raster layer for the AOI	Must be defined projection and located in the AOI
PGA Raster	Raster Layer	PGA raster layer for the AOI	Must be defined projection and located in the AOI
Phase	Value List Options: Phase 1 or 2	Runs the first or second phase of the parameter extraction	Both must be run once before the second tool can be used

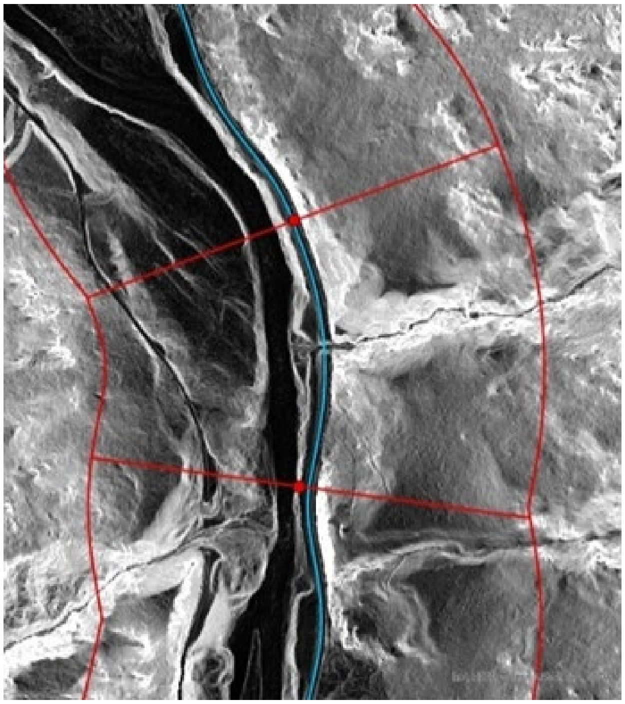

Figure 4.9 Development of perpendicular lines in GIS to extract slope at a Parks Highway site.

4.2.2. Tool 2: RoARS calculations

After the maximum slope and PGA are added to each rock slope entry from the data extraction tool, the second tool – "02_ROARS Analysis" – performs the RoARS calculations from Massey et al. (2022). The second tool requires three inputs (Table 4.3): the Rockslopes layer and associated attributes produced in the first tool, the predicted erosion rate for the rock slopes, and the units of PGA.

Table 4.4 Description of output fields from RoARS calculations is a summary of the calculated RoARS fields. The first field is the "Day1EQRate," which estimates the range for possible rockfall rates that can be triggered at a given slope from a given level of seismic activity (Eqn 4.3). We derived the constants from multi-linear regression statistics using Eqn 4.2, and the constants are in m^3/m^2/day to show the expected volume per rock slope area per day. The dataset used contained the slope height in feet and is automatically converted to meters. The PGA is automatically converted to the appropriate units given the user's input in the tool:

$$Day1EQRate = e^{1.5762*ln(Slope\ Height) + 6.4311*ln(Slope\ Angle) + 0.5258*ln(PGA) - 37.1220} \quad \text{Eqn 4.3}$$

where *Slope Height* is in m, *Slope Angle* is in degrees, PGA_H is m/s^2, and *Day1EQRate* is m^3/m^2/day.

The next field calculated is the factor of increase – "IF_EQ" – which estimates the factor of increase in rockfall activity from the earthquake (EQ) over the baseline activity rate (input by the user) (Eqn 4.4):

$$IF_{EQ} = \frac{Day1EQRate}{BaselineRate} \quad \text{Eqn 4.4}$$

where *Day1EQRate* and *BaselineRate* are both in m^3/m^2/day. Next, the estimated rockfall volume associated directly with the EQ – "VOL_EQ" – is calculated using Eqn 4.5:

$$Vol_{EQ} = IF_{EQ} * BaselineRate * Area \quad \text{Eqn 4.5}$$

where Vol_{EQ} is in m^3, the *BaselineRate* is in m^3/m^2/day, and *Area* is in m^2. The estimated EQ rockfall volume is then normalized by the length along the slope, "Vol_EQ_div_L" (Eqn 4.6):

$$\frac{Vol_{EQ}}{L} = \frac{Vol_{EQ}}{Slope\ Length} \quad \text{Eqn 4.6}$$

where Vol_{EQ}/L is in m^3/m, Vol_{EQ} is in m^3, and *Slope Length* is in m.

Table 4.3 Description of input parameters for Tool "02_ROARS Analysis"

Input Field	Data Type	Description	Notes/Assumptions
Rockslopes Point Layer	Layer	Rock slopes layer that was used in the first tool	Must be run through first tool so that the Max_Slope and PGA fields exist
Erosion Rate (m^3/m^2/day)	Double	Typical erosion rate for the AOI	Must be in m^3/m^2/day
PGA Scale Factor	Value List Options: 100%g, g, m/s^2	Units of the PGA raster	Needed to scale PGA consistently to m/s^2 for RoARS

Table 4.4 Description of output fields from RoARS calculations

Calculated Field	Field Name	Definition	Units
Estimated EQ Rockfall Rate	Day1EQRate	Estimated EQ rockfall rate for Day 1 after the earthquake	$m^3/m^2/day$
Factor of Increase for Earthquake Rockfalls	IF_EQ	Factor of increase in rockfall activity resulting from the EQ over the baseline activity rate	N/A
Factor of Increase for non-Earthquake Rockfalls	IF_NEQ	Factor of increase in non-seismic rockfall activity after the EQ over the baseline activity rate	N/A
Estimated EQ Rockfall Volume	VOL_EQ	Estimated EQ rockfall volume after the EQ	m^3
Estimated EQ Rockfall Volume Normalized by Length	VOL_EQ_div_L	Estimated EQ rockfall volume from the EQ normalized by length along the slope	m^3/m
Factor of Increase based on Lower Estimates	LOWER_IF_NEQ_Day1	Increase in rockfall activity and restoration times using lower bound estimates of geomorphic rates to compute the RoARS coefficients	N/A
Restoration Times (days) based on Lower Estimates	LOWER_T_RESTORE_days		Days
Restoration Times (years) based on Lower Estimates	LOWER_T_RESTORE_years		Years
Factor of Increase based on Upper Estimates	UPPER_IF_NEQ_Day1	Increase in rockfall activity and restoration times using upper estimates of geomorphic rates to compute the RoARS coefficients	N/A
Restoration Times (days) based on Upper Estimates	UPPER_T_RESTORE_days		Days
Restoration Times (years) based on Upper Estimates	UPPER_T_RESTORE_years		Years
Factor of Increase based on Average Estimates	AVG_IF_NEQ_Day1	Increase and restoration times using the average of the RoARS coefficients from the lower and upper estimates of geomorphic rates	N/A
Restoration Times (days) based on Average Estimates	AVG_T_RESTORE_days		Days
Restoration Times (years) based on Average Estimates	AVG_T_RESTORE_years		Years
Factor of Increase in the Non-Earthquake Activity	SUM_IF_NEQ_Day1	Factor of increase in the non-EQ activity rate over baseline conditions on Day 1	N/A
Restoration Times (days)	SUM_T_RESTORE_days	Restoration times to return to baseline rockfall conditions in days. Provided in the format: Average (Lower Estimate-Upper Estimate)	Days
Restoration Times (years)	SUM_T_RESTORE_years	Restoration times to return to baseline conditions in years. Provided in the format: Average (Lower Estimate-Upper Estimate)	Years
Predicted Closure Time (Day 1)	ClosureTime	Closure time based on RIM database correlation	Hours

The non-earthquake (NEQ) rockfall rates and restoration time are calculated using lower, upper, and average estimates of geomorphic rates (Eqn 4.7 and Eqn 4.8) using the different coefficients for lower, upper, and average estimates provided in Table 4.5:

$$(IF_{NEQ}) = (NEQ_{\alpha} * IF_{EQ})^{NEQ_{\beta}} \quad \text{Eqn 4.7}$$

$$(T_{restore,days}) = \left(\frac{1}{(IF_{NEQ})}\right)^{Decay_{\beta}} \quad \text{Eqn 4.8}$$

where IF_{NEQ} is the increase factor for non-seismic rockfall activity, IF_{EQ} is the seismic rockfall activity increase factor, α and β are power-law scaling factors to reflect post-seismic rockfall activity, and $T_{restore,days}$ is the time needed for restoration in days. The results from the previous fields are then displayed in the format of "Average Estimate (Lower Estimate – Upper Estimate)" for the factor of increase in non-earthquake activity (SUM_IF_NEQ_DAY1) and the restoration times (SUM_T_RESTORE).

The last field calculated is the closure time, which is computed using the relationship derived in the RIM database developed in a previous PacTrans project (Holtan 2021) (Eqn 4.9):

$$ClosureTime = 2.9593 * Volume^{0.5399} \quad \text{Eqn 4.9}$$

where *ClosureTime* is in hours, and *Volume* is the VOL_{EQ} term in yd^3.

4.3. Scenario Events

For each study location we considered multiple seismic scenario events (i.e., shakemaps) developed by the Alaska Earthquake Center (AEC) and the United States Geological Survey (USGS) Earthquake Hazards Program (EHP). Table 4.6 is a summary of the details on the respective magnitude and location of these events, Figure 4.10 provides the epicenters of the referenced events, and **Error! Reference source not found.** through**Error! Reference source not found.** are maps of each location and levels of shaking. The first and last scenarios for Long Lake (north-northwest (NNW) Anchorage and Elmendorf Airforce Base (AFB)) were created for the same event but the Elmendorf AFB scenario has been more recently updated. Both shakemaps were included in order to see how the changes between the shakemap models impact the results. Note that "Glitter Gulch" is a colloquialism for Nenana Canyon along the Parks Highway. This has been clarified in multiple places in the following text.

We created estimates of PGA across Alaska for all seismic scenarios using USGS Shakemaps (Wald et al., 1999) (Figure 4.10). Ground shaking can be expressed through intensity, velocity, or acceleration. The magnitude of an earthquake represents the energy it releases while the intensity is a measure of the ground shaking at a particular point. The intensity at a site depends on the location of the epicenter of the earthquake, its magnitude, the rock and soil conditions, and the variations in the propagation of seismic waves (due to the structure of the Earth's crust) (UAF 2020). As part of the TriNet project (Wald

Table 4.5 Restoration time coefficients for lower, upper, and average geomorphic rates from Massey et al. (2022)

	NEQ_{α}	NEQ_{β}	$Decay_{\beta}$
Lower	11.823	0.4157	-0.791
Upper	7.575	0.3757	-0.753
Average	9.699	0.3957	-0.772

Table 4.6 Summary of selected scenario events used in the RoARS regional analysis. SC is scenario, AEC is the Alaska Earthquake Center, and USGS EHP is the USGS Earthquake Hazards Program.

Scenario Name	**Western Denali (Glitter Gulch SC 1)**	**Northern Foothills (Glitter Gulch SC 2)**	**Wadati-Benioff Zone (WBZ) (Glitter Gulch SC 3)**	**Central Alaska (Glitter Gulch SC 4, Long Lake SC 4)**	**NNW Anchorage (Long Lake SC 1)**	**Prince William Sound "The Great Alaska Earthquake" (Long Lake SC 2)**	**Southern Alaska (Long Lake SC 3)**	**Elmendorf AFB (Long Lake SC 4)**
Source	AEC	AEC	AEC	USGS EHP	USGS EHP	USGS EHP	USGS EHP	AEC
Event or Scenario	Scenario	Scenario	Scenario	Event: 11/03/2002	Event: 11/30/2018	Event: 03/28/1964	Event: 11/03/1943	Event: 11/30/2018
Run Name	GG1	GG2	GG3	B1-GG4 B1-LL4	LL1	LL2	LL3	LL4
Link	Link	Link	Link	Link	Link	Link	Link	Link
Location	N63.47 W148.40	N63.71 W149.50	N63.85 W149.10	N63.514 W147.453	N61.346 W149.955	N60.908 W147.339	N61.776 W151.051	N61.35 W149.96
Magnitude	7.2	7.1	7.1	7.8	7.1	9.2	7.6	7.1
Depth (km)	10.0	10.0	125.0	4.2	46.7	25.0	15.0	46.7
Max PGA (%g)	0.740	0.740	0.317	0.735	0.376	0.985	0.321	0.363
Max PGA for Study Sites (%g)	0.632	0.703	0.286	0.140	0.046	0.220	0.269	0.081
Average PGA for Study Sites (%g)	0.322	0.359	0.272	0.119	0.030	0.097	0.199	0.045
Std. Dev. For Study Sites	0.188	0.217	0.014	0.001	0.001	0.004	0.002	0.000

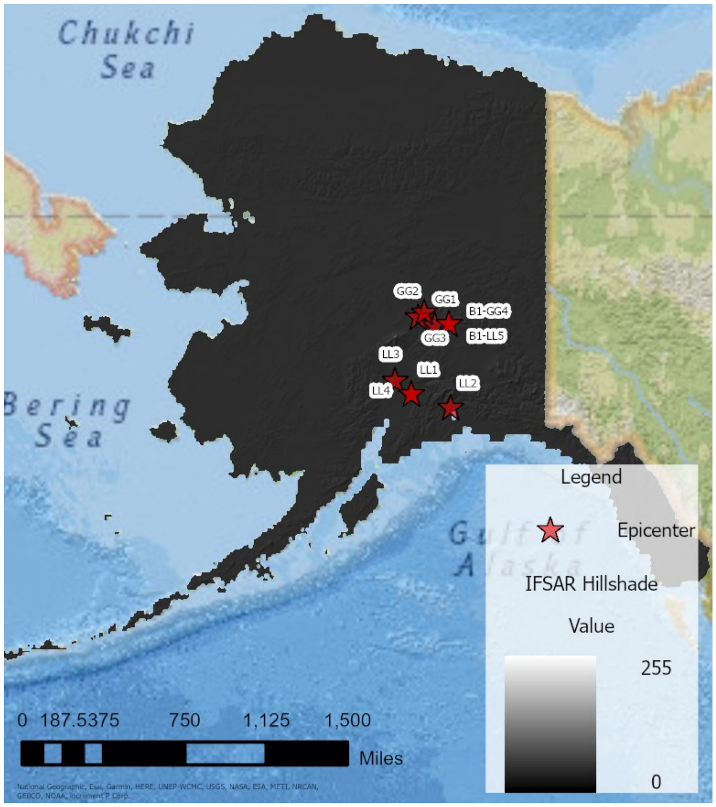

Figure 4.10 Map of epicenters for scenario events

et al., 1999), a seismic network was developed that can calculate and map the measured ground acceleration and velocity within five minutes of an earthquake. The AEC and USGS provide both post-earthquake shakemaps as well as plausible “Earthquake Scenarios” occurring along faults that have a history of rupturing and are expected to rupture in the future. The shakemaps vary in spatial resolution but are primarily created to display general trends with a range of 30” to 2’ arcgrid resolution. Shakemaps can improve emergency response systems but are by no means earthquake predictions. Although the magnitude or day of an earthquake is unpredictable, understanding the anticipated shaking and associated impacts of an earthquake can greatly improve earthquake scenario planning and preparedness.

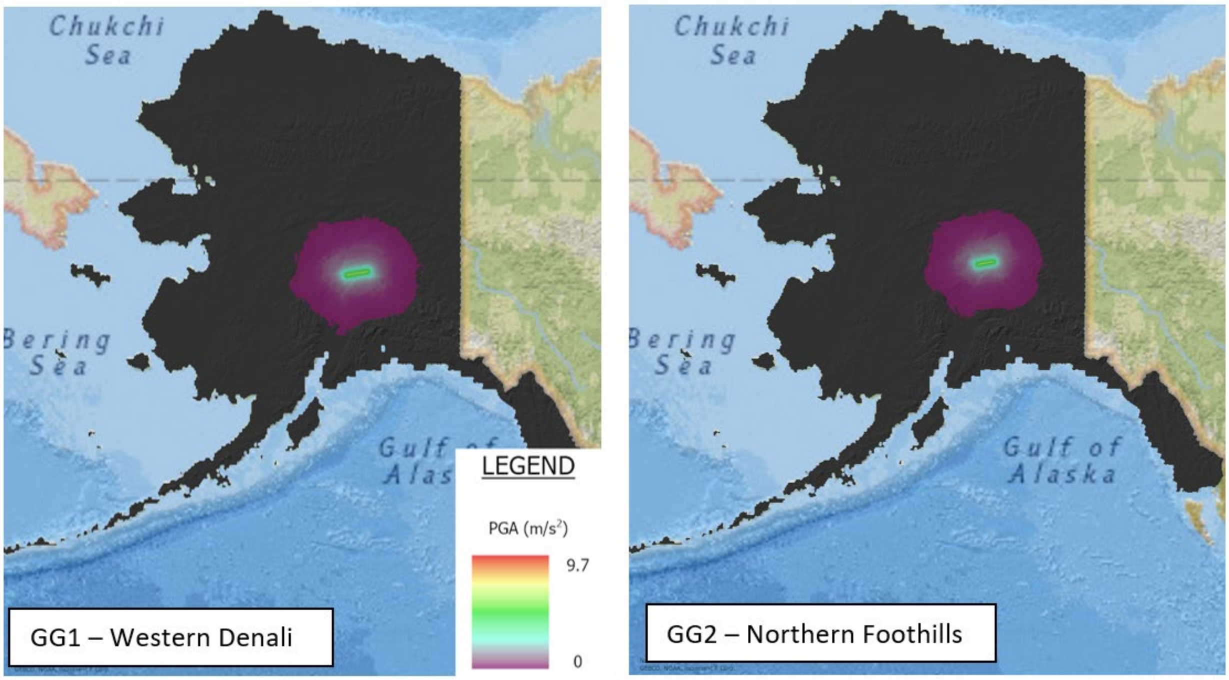

Figure 4.11 Glitter Gulch (Nenana Canyon) Scenarios 1 and 2. Note that the same PGA legend also applies to Figure 4.12-Figure 4.14.

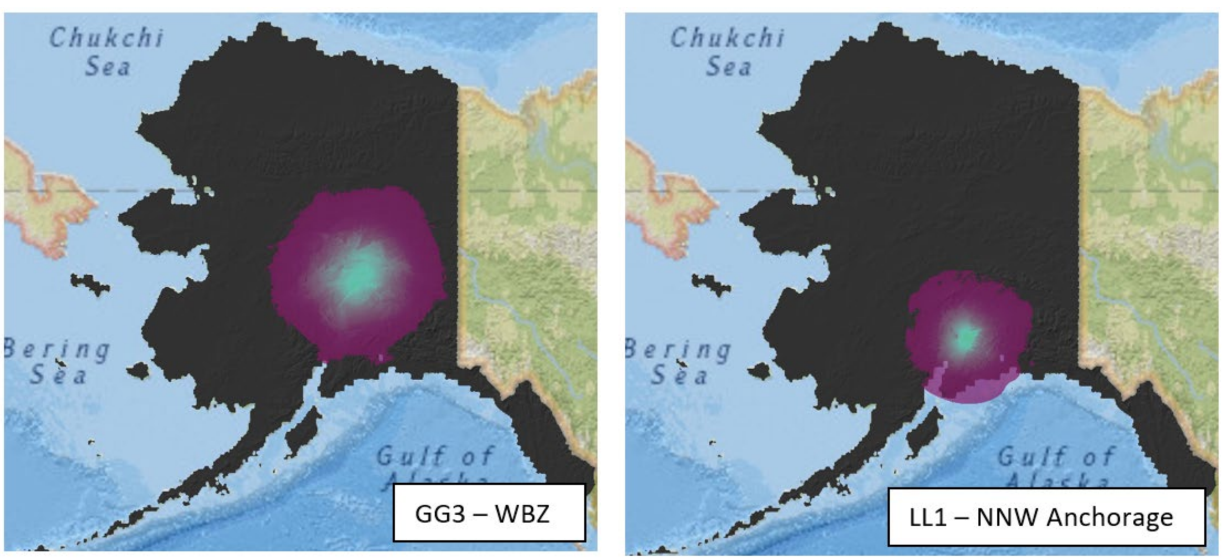

Figure 4.12 Glitter Gulch (Nenana Canyon) Scenario 3 and Long Lake Scenario 1

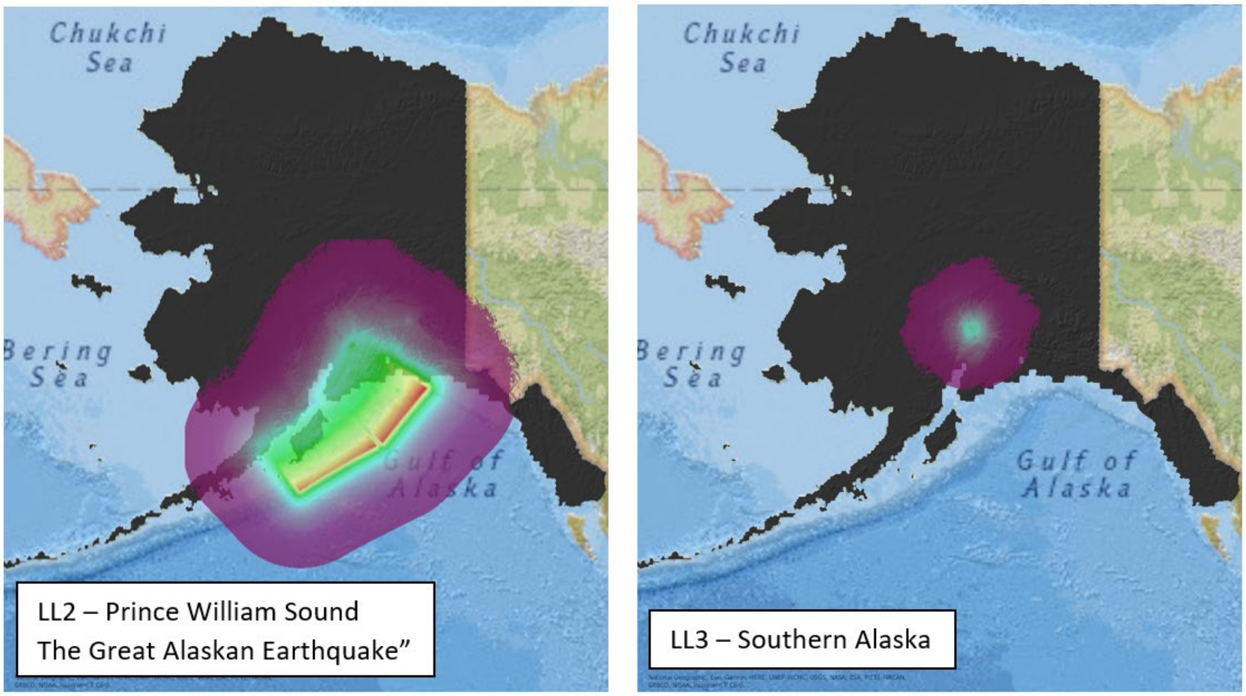

Figure 4.13 Long Lake Scenarios 2 and 3

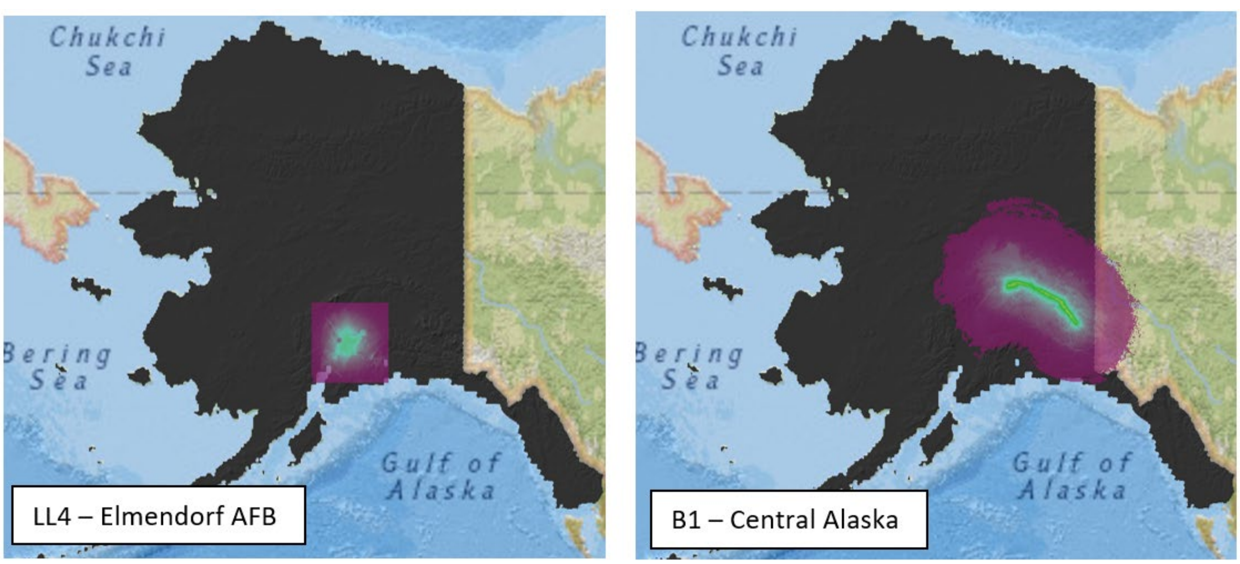

Figure 4.14 Long Lake Scenario 4 and both Glitter Gulch (Nenana Canyon) and Long Lake Scenarios 1

4.4. Regional Analysis Results

Table 4.7 is a summary of the statistics for attributes extracted for the rock slopes within each study area, Glitter Gulch (Nenana Canyon) and Long Lake. We ran each shakemap scenario individually through the 01_Parameter Extraction tool, resulting in nine distinct outputs. Next, each scenario was run through the 02_ROARS Analysis tool resulting in erosion rates of 8.456 x 10^{-5} m^2/s^2/day and 1.9286 x 10^{-5} m^2/s^2/day for Glitter Gulch (Nenana Canyon) and Long Lake sites, respectively (as determined from repeat TLS epochs collected during previously-supported PacTrans research). The main outputs on which we focused were Volume and Average Restoration Time (days).

4.4.1. Glitter Gulch (Nenana Canyon)

In the first scenario for Glitter Gulch (Nenana Canyon), Western Denali (Figure 4.15), the area that has the highest PGA encapsulates about a third of the rock slopes; however, only one of the rock slopes in that area had a large volume (10,900 m^3). None of the three rock slopes with the highest PGA experienced the expected high volume as a result of higher PGA. Similarly, some of the highest volumes occur further from the epicenter in rock slopes associated with lower PGA values. Also, the rock slopes with larger earthquake failure volumes did not consistently have higher restoration times.

In the second scenario for Glitter Gulch (Nenana Canyon), Northern Foothills (Figure 4.16), the epicenter was more centered over the sites, with a slightly larger PGA at the epicenter than the first scenario. All of the rock slopes had notably higher volume predictions than the first scenario. The range of volume

Table 4.7 Study site statistics

Statistic		**Glitter Gulch (Nenana Canyon)**	**Long Lake**
Slope (°)	Minimum	37.1	33.9
	Maximum	71.1	84.1
	Average	54.6	60.9
	Standard Deviation	12.2	11.5
Height (ft)	Minimum	20	12
	Maximum	1,200	830
	Average	205	84.7
	Standard Deviation	331	130
Length (ft)	Minimum	85	32
	Maximum	2,200	6,010
	Average	805	775
	Standard Deviation	738	884
Area (ft^2)	Minimum	1,930	1,090
	Maximum	881,000	820,000
	Average	195,000	52,400
	Standard Deviation	329,000	114,000

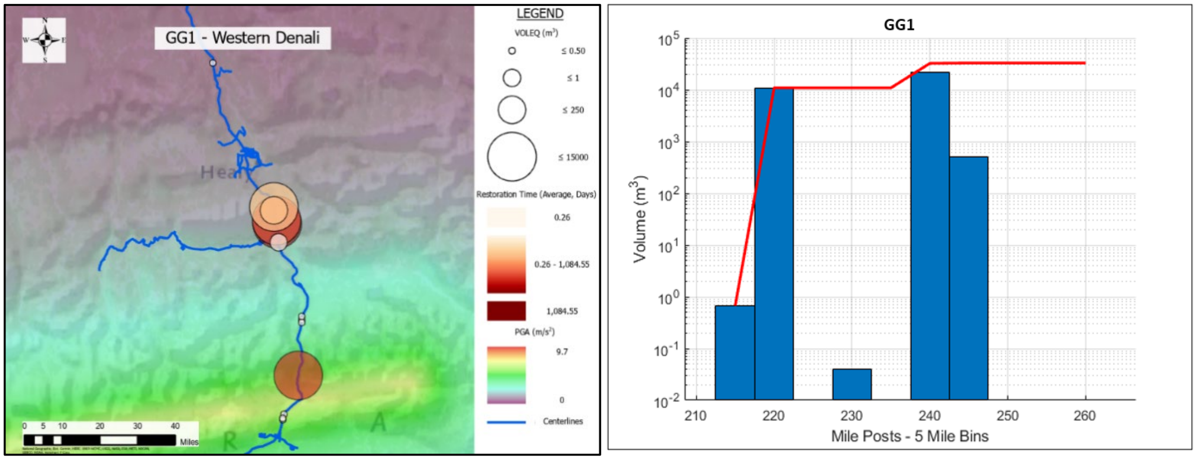

Figure 4.15 Glitter Gulch Scenario GG1 results (accumulated volume in red in panel to the right)

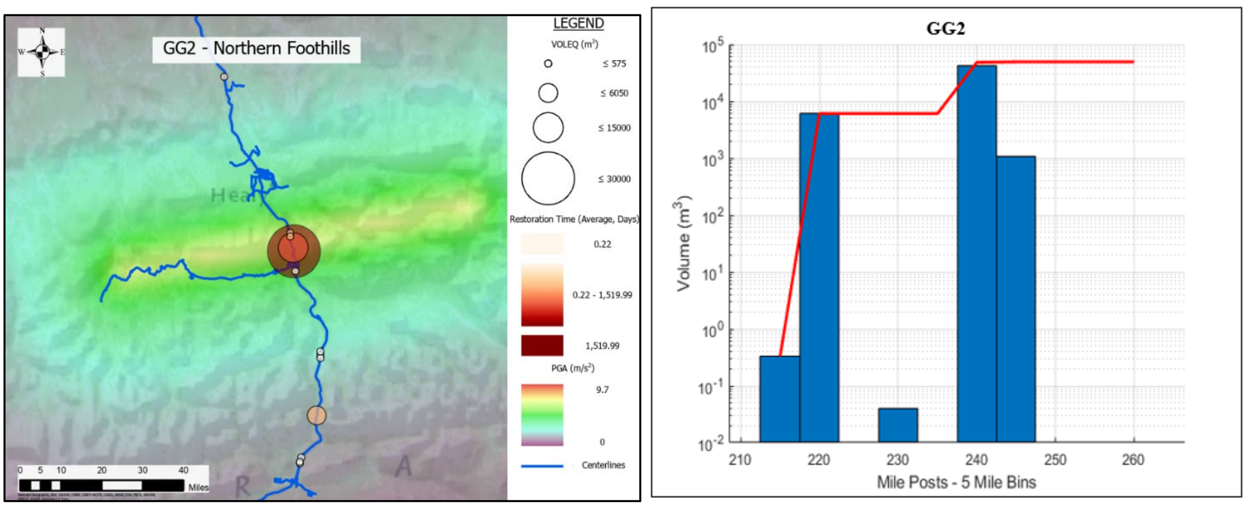

Figure 4.16 Glitter Gulch Scenario GG2 results (accumulated volume in red in panel to the right)

predictions was larger with the highest being around 30,000 m^3 versus a range of 15,000 m^3 for the first scenario. In this scenario, the larger volume predictions had proportional restoration times, unlike the first scenario where large volume estimations did not always result in high restoration times.

For the third Glitter Gulch (Nenana Canyon) scenario (Figure 4.17), every rock slope had approximately the same PGA, ranging from ~26 %g to ~29 %g. Therefore, the differences in volume and restoration time were primarily due to the differences in rock slope geometry. Similar to the previous two scenarios, the bulk of the high-volume predictions fell around MP 220-225 or MP 240-250. The average restoration time varied similarly to the other two scenarios, with a range of approximately 0.24 – 1200 days (Western Denali - 0.26 – 1,100 days; Northern Foothills - 0.22 – 1,500 days). It is somewhat surprising that all had similar restoration time ranges when the second scenario (Northern Foothills) had a higher average PGA overall.

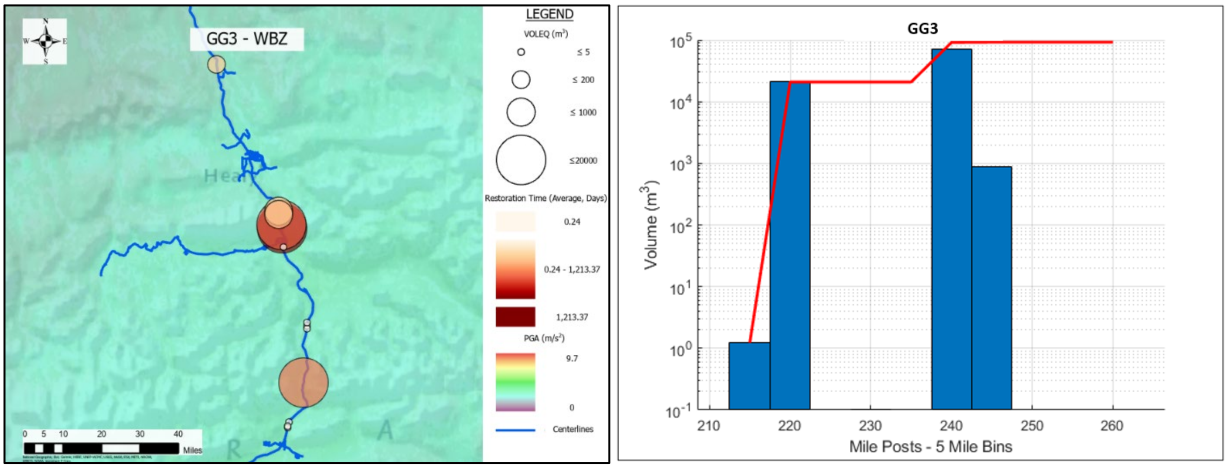

Figure 4.17 Glitter Gulch Scenario GG3 results (accumulated volume in red in panel to the right)

The final scenario for Glitter Gulch (Nenana Canyon), Central Alaska (Figure 4.18), had the lowest average PGA of the sites, but similar volume outputs as the first scenario (Western Denali), with both peaking at less than 15,000 m^3. The restoration times had a smaller range to the other scenarios, peaking at nearly 1,000 days.

Overall, among all four scenarios for Glitter Gulch (Nenana Canyon), the same sections of the road tended to have higher volume estimates failing around MP 220-225 or MP 240-250. Although this may seem counterintuitive because the PGAs for these different scenarios are so different, it can be concluded that the rock slope geometry largely contributes to the volume estimations (given that the PGA is above a triggering threshold of approximately 10% g). Another interesting trend is that the restoration times for each rock slope are similar between all of the scenarios, regardless of the variation in seismic activity.

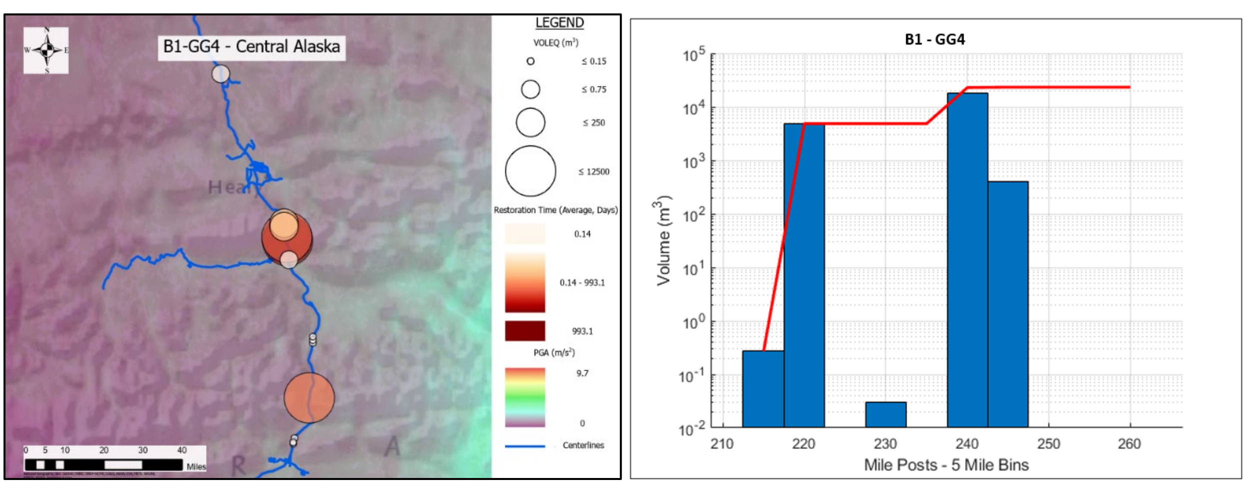

Figure 4.18 Glitter Gulch Scenario B1 - GG4 results (accumulated volume in red in panel to the right)

4.4.2. Long Lake

The results for Long Lake were significantly different than Glitter Gulch (Nenana Canyon), largely due to the lack of high seismic activity near the rock slopes of interest. The shakemaps tended to have epicenters further from the majority of the rock slopes as compared to Glitter Gulch (Nenana Canyon).

For Long Lake Scenario 1, NNW Anchorage (Figure 4.19), the larger volume estimates tended to occur near the higher PGA areas; however, the largest volume estimates were not necessarily at the points of highest PGA. Typically, the larger volume estimates fell within MP 55 to 90, with the largest within MP 70 - 85. Similar to the Glitter Gulch (Nenana Canyon) results, the higher average restoration time in days did not necessarily correspond with higher volume estimations. This occurs since active sites will tend to produce higher volumes but return to baseline levels quickly because of how active they are without coseismic events. Because the increase from the earthquake is proportionally larger at less active sites, they take longer to resume baseline levels.

For Scenario 2 Prince William Sound (Figure 4.20), the results were significantly different than the NNW Anchorage results. For the first scenario, the majority of large volume estimations fell within MP 55 to 90, while in the second scenario, the majority of high-volume estimations were in MP 90 - 110. In the second scenario, the PGA was typically higher than that of the first scenario with a smaller range overall, resulting in the volume being more dependent on rock slope geometry.

In the third scenario Southern Alaska (Figure 4.21), the PGA was low, with all of the results being dependent on the rock slope geometry instead of the PGA. Compared to the other scenarios, this scenario had the smallest standard deviation with the smallest average PGA, and overall the smallest predicted volume and restoration time.

The fourth scenario, Elmendorf (Figure 4.22), had similar results to the first scenario. The range of volume estimates and restoration times, and the average PGA were almost the same between the two scenarios. The biggest difference was that the fourth scenario had a higher standard deviation of PGA than the first scenario, resulting in some of the rock slopes having lower volumes in the fourth scenario than the first. Both scenarios have the most activity within MP 55 - 90 but the volumes were not the same between the two scenarios.

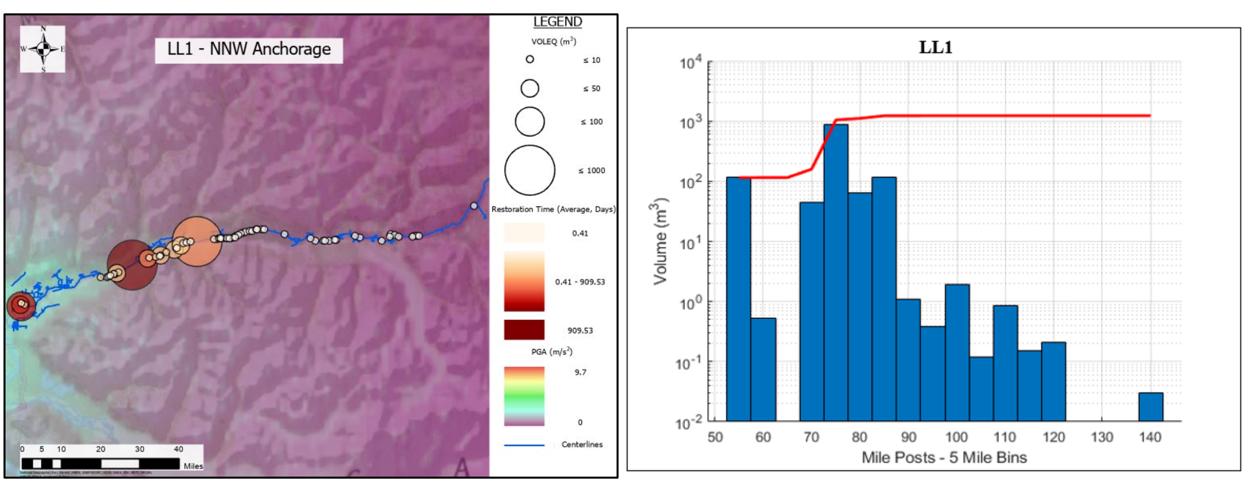

Figure 4.19 Long Lake Scenario LL1 results (accumulated volume in red in the panel to the right)

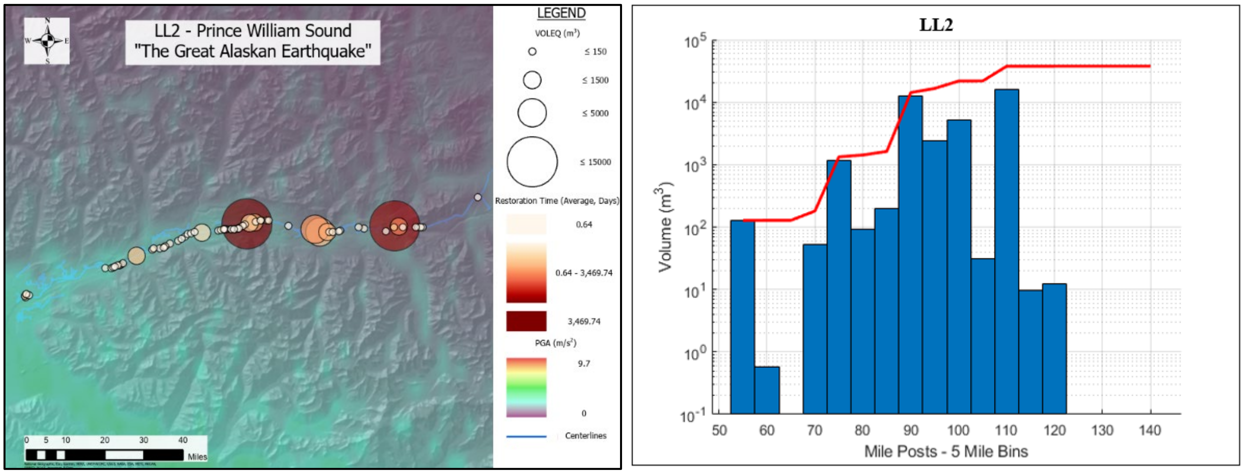

Figure 4.20 Long Lake Scenario LL2 results (accumulated volume in red in panel to the right)

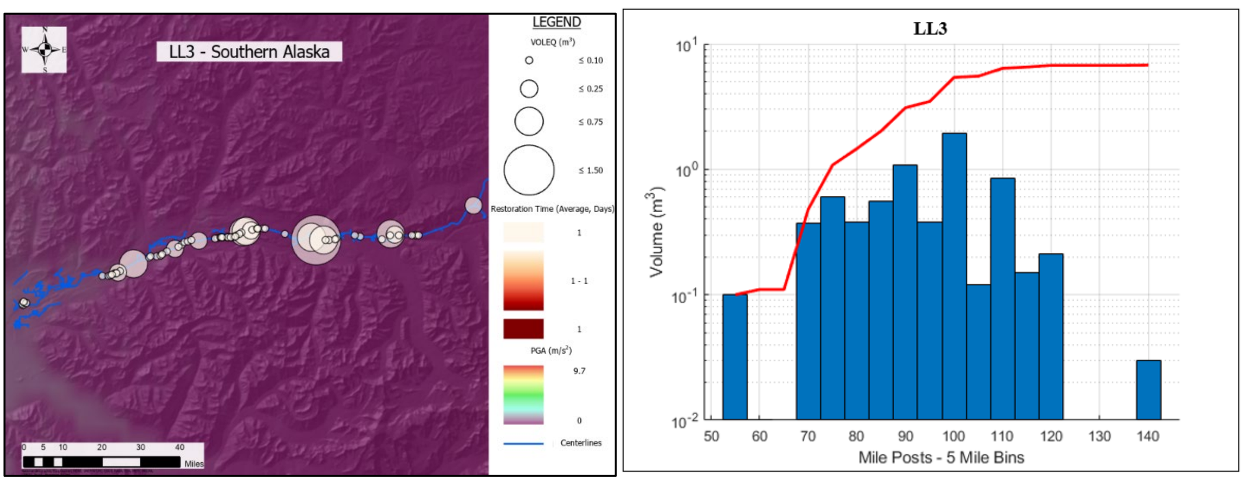

Figure 4.21 Long Lake Scenario LL3 results (accumulated volume in red in panel to the right)

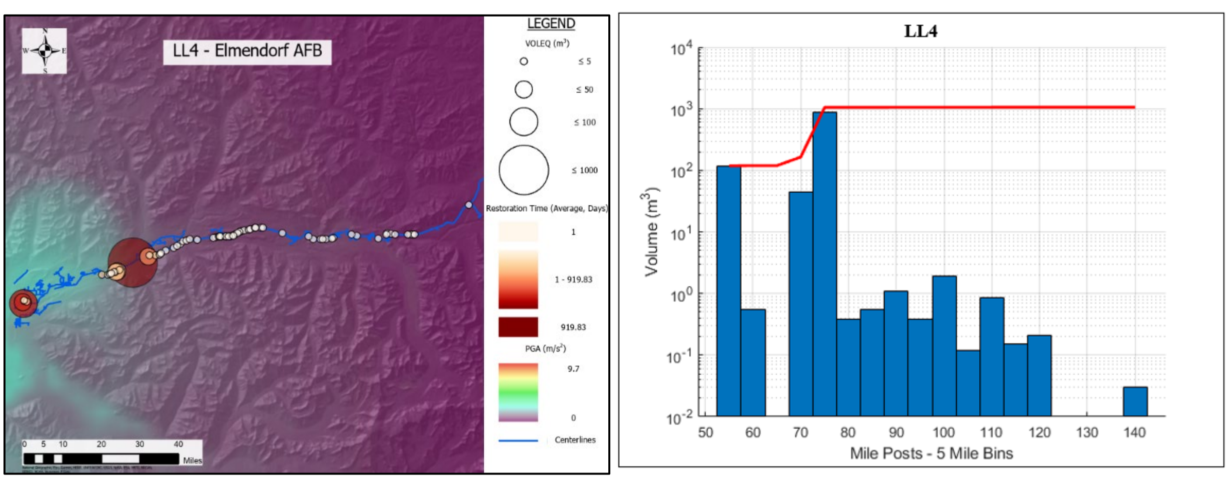

Figure 4.22 Long Lake Scenario LL4 results (accumulated volume in red in panel to the right)

The fifth scenario (Figure 5.23), Central Alaska, produced results similar to the third scenario. Both scenarios had small PGAs overall and therefore resulted in small volume estimates and restoration times.

Overall among all of the Long Lake scenarios, PGA played a larger role than geometry in the predicted volume. Larger volume estimates tended to correlate with higher PGAs, whereas in the Glitter Gulch (Nenana Canyon) area, the same rock slopes had higher volumes regardless of the seismic event. The variation in total volume is smaller in Glitter Gulch than in Long Lake, even though there was a wider range of seismic activity in the latter (Table 4.6). This could be due to the variability in geometry at Glitter Gulch as compared to Long Lake. Long Lake has more consistent geometry (Table 4.7) with significantly smaller standard deviations for the area and height than Glitter Gulch. Long Lake also has more rock slopes distributed across the section, whereas Glitter Gulch has some large slopes but at distinct locations.

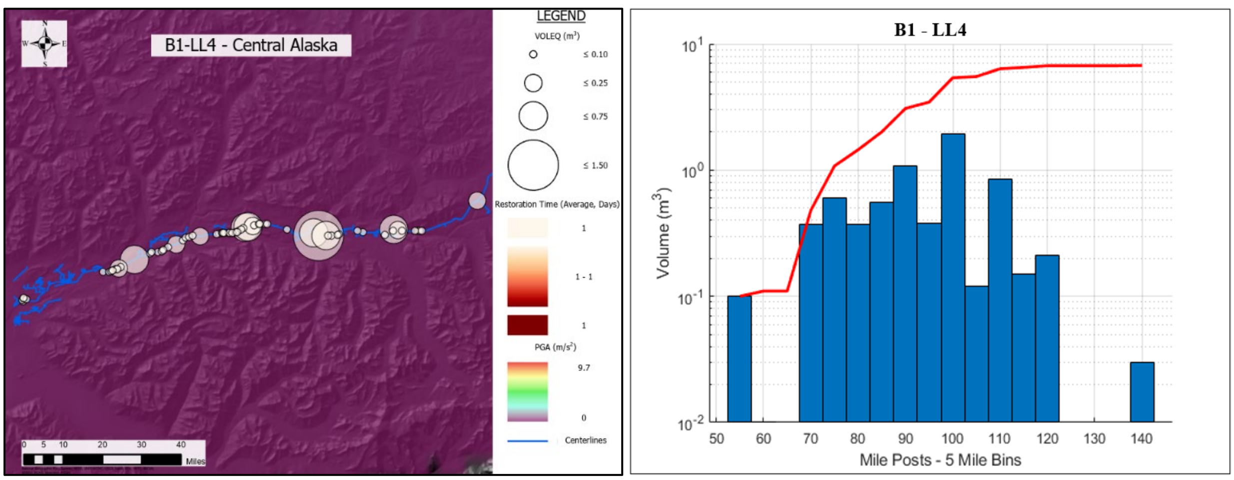

Figure 4.23 Long Lake Scenario B1-LL4 results (accumulated volume in red in panel to right)

CHAPTER 5. SUMMARY AND CONCLUSIONS

Transportation corridors rely on maintenance and quick emergency responses in order to serve the public; however, the climate, geology, and topography of the Pacific Northwest often challenges local transportation agencies in their ability to maintain roadway efficiency. There are many geohazards to mitigate, including landslides, rockfall, debris flows, and general slope instability. These events are common but can be unpredictable and may result in devasting damage to the transportation infrastructure, becoming risks to motorists. Unexpected hazards often force motorists to use large detours on roads that cannot always accommodate the increased traffic capacity. Furthermore, the mitigation efforts and maintenance necessary to repair roadways after geohazards occur can take anywhere from hours to months to complete, oftentimes resulting in the complete loss of the old roadways and decreased capacity during repairs. In this study, we developed a method to apply the RoARS methodology to large sections of roadways, therefore providing transportation planners and engineers with the information to make quantitatively-informed decisions regarding the potential repairs and maintenance that might be needed.

Applying the RoARS methodology illustrated that regardless of the variation in seismic activity, restoration times of rock slopes remained similar between scenarios. This is expected because more active rock slopes have a higher likelihood of producing high volumes of debris and while their post-earthquake rockfall rate could still be high, they are likely similar to the pre-earthquake rockfall rates. Similarly, for all the scenarios tested, the same sections of road tended to have higher volume estimates. This is useful because it shows that rock slope size is likely a stronger control on rockfall volumes than seismic activity. Note that the Long Lake study section did not as clearly display this trend because the geometries of the slopes were so similar. Therefore, even with limited scenarios to test, transportation agencies can use this methodology to understand the general risk of each rock slope under a seismic event. While it can be difficult to predict the time, location, and magnitude of seismic events, applying the RoARS methodology can at least provide transportation agencies quantitative insight towards which rock slopes should be prioritized in terms of mitigation. Overall, this research helps to identify the routes that are the most vulnerable to closures due to landslides and rockfalls, and allows transportation professionals to create effective plans to mitigate these closures quickly.

Several publications resulted from this work, including an MS thesis (Holtan 2021), conference papers and presentations (Olsen et al. 2022, Olsen et al. *In Press*), and a journal paper (Massey et al. 2022).

CHAPTER 6. REFERENCES

Alaska Department of Transportation and Public Facilities (ADOT&PF). (2020). Alaska DOT&PF Route Centerlines. Fairbanks, Alaska Department of Transportation and Public Facilities. Available from: < https://dot.alaska.gov/stwddes/gis/shapefiles.shtml>

Alaska Geospatial Council (AGC). (2020). Alaska Coastline Shapefiles. Fairbanks, Alaska Geospatial Office. Available from: < https://gis.data.alaska.gov/search?q=alaska%20boundary >

ASTM International. (2007). *Standard Test Method for Determination of the Point Load Strength Index of Rock and Application to Rock Strength Classifications, D5731-07:* ASTM International, West Conshohocken, PA, 11 p.

ASTM International. (2014). *Standard Test Method for Determination of Rock Hardness by Rebound Hammer Method, D5873-14:* ASTM International, West Conshohocken, PA, 6 p.

Attewell, P.B., and Farmer, I W. (1976). *Principles of Engineering Geology*: Chapman and Hall, London.

Csejtey, Jr., B., Mullen, M. W., Cox, D. P., Gilbert, W. G., Yeend, W. E., Smith, T. E., Wahrhaftig, C., Craddock, C., Brewer, W. M., Sherwood, K. W., Hickman, R. G., Stricker, G. D., St. Aubin, D. R., Goerz, D. J., 1986. *Geology and Geochronology of the Healy quadrangle, Alaska*: United States Geological Survey, Open-File Report 86-396, 92 p., 4 sheets, scale 1:250,000.

Del Gaudio, V., and Wasowski, J., 2004. Time probabilistic evaluation of seismically induced landslide hazard in Irpinia (Southern Italy). *Soil Dynamics and Earthquake Engineering,* 24.12: 915-928.

Dunham, L., Wartman, J., Olsen, M. J., O'Banion, M. S., Cunningham, K., 2017. Rockfall Activity Index (RAI): a lidar-derived, morphology-based method for hazard assessment. *Engineering Geology,* 221: 184-192.

Frankel, A. D., Wirth, E. A., Marafi, N., Vidale, J. E., Stephenson, W. J., 2018. Broadband synthetic seismograms for magnitude 9 earthquakes on the Cascadia megathrust based on 3-D simulations and stochastic synthetics, part 1: methodology and overall results. *Bulletin of the Seismological Society of America*, 108(5A): 2347-2369.

Goldfinger, C., Nelson, C., Morey, A., Johnson, J., Patton, J., Karabanov, E. B., Gutierrez-Pastor, J., Eriksson, A. T., Gracia, E., Dunhill, G., Enkin, R.J. Dallimore, A., Vallier, T., 2012. *Turbidite Event History--Methods and Implications for Holocene Paleoseismicity of the Cascadia Subduction Zone*: Professional Paper 1661-F, U.S.Geological Survey, Available at: <https://doi.org/10.3133/pp1661F>

Holtan, K., 2021. *Assessing Seismic Rockfall Impacts on Mobility in Transportation Corridors*: MS Thesis, Oregon State University, 105 p.

Jibson, R. W., and Harp, E. L., 2016. Ground motions at the outermost limits of seismically triggered landslides. *Bulletin of the Seismological Society of America*, 106(2): 708-719.

Litchfield, N. J., Van Dissen, R. J., Massey, C. I., 2016. *Pre-Christchurch Earthquake Sequence Rockfalls in the Port Hills, Christchurch: Wakefield Avenue Trench*: Report 2016/25iii, 32 p. GNS Science, Lower Hutt, N.Z.

Mason, D., Brabhaharan, P., Saul, G., 2017. Performance of road networks in the 2016 Kaikōura earthquake: observations on ground damage and outage effects. *Proc., 20th Symposium of the New Zealand Geotechnical Society:* Napier, New Zealand, November 24-26, 2017.

Massey, C. I., McSaveney, M. J., Richards, L., 2015. Characteristics of some rockfalls triggered by the 2010/2011 Canterbury earthquake sequence, New Zealand. *Engineering Geology for Society and Territory - Volume 2: Landslide Processes*, 1943-1948. doi:10.1007/978-3-319-09057-3_344

Massey, C. I., McSaveney, M. J., Taig, T., Richards, L., Litchfield, N. J., Rhoades, D. A., McVerry, G. H., Lukovic, B., Heron, D. W., Ries, W., Van Dissen, R. J., 2014. Determining rockfall risk in Christchurch using rockfalls triggered by the 2010–2011 Canterbury earthquake sequence. *Earthquake Spectra*: 30(1), 155-181.

Massey, C.J., Olsen, M.J., Wartman, J., Senogles, A., Lukovic, B., Leshchinsky, B.A., Archibald, G., Litchfield, N., Van Dissen, R., de Vilder, S., Holden C., 2022. Rockfall activity rates before, during, and after the 2010/11 Canterbury Earthquake Sequence. *Journal of Geophysical Research: Earth Surface,* 127, e2021JF006400, https://doi.org/10.1029/2021JF006400

Olsen, M.J., Massey, C., Holtan, K., Wartman, J., Leshchinsky, B., Darrow, M., Senogles, A., 2022. Application of the rockfall activity rate system, RoARS. *Extended Abstract in Proceedings of the International Society for Rock Mechanics and Rock Engineering, Eurock 2022*: Helskinki, Finland, 12-15 September, 2022.

Olsen, M. J., Massey, C., Leshchinsky, B., Wartman, J., Senogles, A. (*In Press*). Forecasting post-earthquake rockfall activity, *Journal of Applied Geodesy, Special Issue: Joint Symposium on Deformation Monitoring.*

Olsen, M. J., Massey, C., Senogles, A., Leshchinsky, B. A., Wartman, J., 2020. *Predicting Seismic-Induced Rockfall Hazard for Targeted Site Mitigation*: Oregon Department of Transportation Research Section and the Federal Highway Administration, SPR-809, 378 p.

Olsen, M.J., Senogles, A., Leshchinsky, B., Massey, C., Archibald, G., Wartman J., 2019. Rockfall activity rates following the Canterbury New Zealand Earthquake. *Proc. 7th International Conference on Geotechnical Earthquake Engineering, 7ICEGE*: Roma Italy, June 2019, p. 4210.

Trop, J. M., Cole, R. B., Sunderlin, D., Hults, C., Todd, E., 2015. Bedrock geology of the Glenn Highway from Anchorage to Sheep Mountain, Alaska – Field Trip Guide. *Geological Society of America* and *Alaska Geological Society*, 46 p. Available at: <https://www.researchgate.net/publication/279850370_Bedrock_geology_of_the_Glenn_Highway_from_Anchorage_to_Sheep_Mountain_Alaska_-_Field_Trip_Guide>

Turner, A. K. and Schuster, R. L. (Eds.), 2012. *Rockfall: Characterization and Control*: Transportation Research Board, 658 p.

University of Alaska Fairbanks (UAF), 2020. ShakeMaps: Alaska Earthquake Center. *Alaska Earthquake Center.* Available at: <earthquake.alaska.edu/earthquakes/shakemaps>

Wald, D. J., Quitoriano, V., Heaton, T. H., Kanamori, H., Scrivner, C. W., Worden, C. B., 1999. TriNet “ShakeMaps”: rapid generation of peak ground motion and intensity maps for earthquakes in southern California. *Earthquake Spectra*, 15(3): 537-555, https://doi.org/10.1193/1.1586057

West, M. E., Bender, A., Gardine, M., Gardine, L., Gately, K., Haeussler, P., Hassan, W., Meyer, F., Richards, C., Ruppert, N. A., Tape, C., Thornley, J., Witter, R. C., 2020. The 30 November 2018 M_w 7.1 Anchorage Earthquake. *Seismological Research Letters*, 91(1), 66-84, doi:10.1785/0220190176

Wilson, F. H., Hults, C. P., Mull, C. G., Karl, S. M., 2015. *Geologic Map of Alaska,* U.S. Geological Survey Scientific Investigations Map 3340, 196 p., 2 sheets, scale 1:1,584,000, https://alaska.usgs.gov/science/geology/state_map/interactive_map/AKgeologic_map.html

Wilson, R. C. and Keefer, D. K., 1985. Predicting areal limits of earthquake-induced landsliding. In *Evaluating Earthquake Hazards in the Los Angeles Region – An Earth-Science Perspective,* Ziony, J.I. (Ed.), U.S. Geological Survey Professional Paper 1360, 317-345.

Wyllie, D. C., and Mah, C. W., 2004. *Rock Slope Engineering: Civil and Mining* (4th *Ed*.). New York: CRC Press, 456 p.

APPENDIX

This appendix contains the two python scripts developed for the analysis.

A.1 Python Script: 01_Parameter Extraction

```
import arcpy
import math

# Need to get parameters ready for use
Rockslopes_Point_Layer =arcpy.GetParameterAsText(0)
Centerlines = arcpy.GetParameterAsText(1)
RunNumber = arcpy.GetParameterAsText(3)
Perpendicular_Lines
=arcpy.GetParameterAsText(2)+"\\"+RunNumber+"_1_PERPLines"
GDB = arcpy.GetParameterAsText(2)
DTM_Mosaic = arcpy.GetParameterAsText(4)
PGA_Raster = arcpy.GetParameterAsText(5)
Phase = arcpy.GetParameterAsText(6)

if Phase == "Phase 1":

    # Make perpendicular lines from centerlines to rockfall points
    points = Rockslopes_Point_Layer
    sr = arcpy.Describe(points).spatialReference # get CRS
    lines = Centerlines
    out_lines = [] # output list
    line_geom = [i[0] for i in
arcpy.da.SearchCursor(lines,'SHAPE@',spatial_reference=sr)] # the road
feature
    with arcpy.da.SearchCursor(points,'SHAPE@') as cursor: # loop through
points
     for row in cursor:
      end = line_geom[0].queryPointAndDistance(row[0])[0].centroid
      # get nearest point on line
      start = row[0].centroid
      out_lines.append(arcpy.Polyline(arcpy.Array([start,end]),sr)) # connect
the dots and add to line list
    arcpy.CopyFeatures_management(out_lines,Perpendicular_Lines) # write line
list to disk

    # BUFFER 200-500 meters
    buffer =
arcpy.GetParameterAsText(2)+"\\"+RunNumber+"_2_Centerlines_Buffer"
    arcpy.analysis.Buffer(Centerlines, buffer, "500 Meters", "FULL", "ROUND",
"ALL")

    # change buffer to polyline
    PLine_buffer =
arcpy.GetParameterAsText(2)+"\\"+RunNumber+"_3_Centerlines_Buffer_PLINE"
    arcpy.management.PolygonToLine(buffer, PLine_buffer)

    # merge perpendicular lines layer and buffer layer
    inputs = [Perpendicular_Lines, PLine_buffer]
    output = arcpy.GetParameterAsText(2)+"\\"+RunNumber+"_4_MergePerpBuffer"
    arcpy.management.Merge(inputs, output, "", "ADD_SOURCE_INFO")
```

```
    # extend perpendicular lines to buffer
    in_features = output  # output from merged layer
    arcpy.edit.ExtendLine(in_features, "5000 meters", "EXTENSION")

    # calculate slope from DTM
    in_raster = DTM_Mosaic
    out_raster = GDB+"\\"+RunNumber+"_5_SlopeRaster"
    out_measurement = "DEGREE"
    z_factor = 1
    method = "PLANAR"
    z_unit = ""
    # slope = arcpy.sa.Slope(in_raster, out_raster, z_factor, method, z_unit)
    # slope.save(out_raster)
    Slope = arcpy.sa.Slope(in_raster=DTM_Mosaic, output_measurement="DEGREE",
z_factor=1, method="PLANAR",
                                   z_unit="METER")
    Slope.save(out_raster)

    # zonal statistics
    in_zone_data = output # merged layer with extended perp lines
    zone_field =  "OBJECTID"
    in_value_raster = out_raster # slope layer from slope step
    statistics_type = "MAXIMUM"
    ignore_nodata = "DATA"
    output_raster_a = GDB+"\\"+RunNumber+"_6_ZonalStatsRaster"
    Zonal = arcpy.sa.ZonalStatistics(in_zone_data, zone_field,
in_value_raster, statistics_type, ignore_nodata)
    Zonal.save(output_raster_a)

    # Extract Multivalues to Points:
    Max_Slope = [output_raster_a, "Max_Slope"]
    new_rockslopes =
arcpy.sa.ExtractMultiValuesToPoints(in_point_features=Rockslopes_Point_Layer,
in_rasters=[Max_Slope], bilinear_interpolate_values="NONE")

else:
    PGA = [PGA_Raster, "PGA"]
    new_rockslopes =
arcpy.sa.ExtractMultiValuesToPoints(in_point_features=Rockslopes_Point_Layer,
in_rasters=[PGA], bilinear_interpolate_values="BILINEAR")
```

A.2 Python Script: 02_ROARS Analysis

```
import arcpy
import math

# Need to get parameters ready for use
Rockslopes_Point_Layer =arcpy.GetParameterAsText(0)
BaselineRate = arcpy.GetParameterAsText(1)

# convert PGA
inTable = Rockslopes_Point_Layer
fieldname = "PGA_Conv"
expression = "PGA_Conv_Function(!PGA!)"
codeblock = """
def PGA_Conv_Function(PGA):
    PGA_UNCONVERTED = float(PGA)
    PGA = math.exp(PGA_UNCONVERTED)

    return float(PGA)
"""
# Calculate the field
arcpy.CalculateField_management(inTable, fieldname, expression, "PYTHON3",
codeblock, "FLOAT")


# 1) Day1EQRate Cals
# Set variables for field calculations
inTable = Rockslopes_Point_Layer      # table containing the field that will
be updated with the new calculation
fieldname = "Day1EQRate"    # field that will be updated (created if it does
not already exist)
expression = "Day1EQRate_Function(!MSHeigtN!, !PGA!, !PGA_Conv!,!Max_Slope!)"
# call calculation function
codeblock = """
def Day1EQRate_Function(SlopeHeight, PGA, PGA_Conv, SlopeAngle):
    BaselineRate = arcpy.GetParameterAsText(1)
    SlopeHeight_UNCONVERTED = SlopeHeight

    # constants for calculations
    C_Hmax = 1.5762
    C_alpha = 6.4311
    C_PGA = 0.5258
    C_Intercept = -37.1220
    YieldAcceleration = 1.0          # constant

    # unit conversions
    SlopeHeight_Converted = SlopeHeight_UNCONVERTED*0.3048        # convert
from feet to meters


    # PGA conversions
    PGA_ScaleFactor = arcpy.GetParameterAsText(2)
    if PGA < 0:
        PGA_UNCONVERTED = float(PGA_Conv)
        PGA = PGA_UNCONVERTED*9.81
    else:
```

```
        PGA_UNCONVERTED = float(PGA)
        if PGA_ScaleFactor == "100% g":                     # convert to
proper units for roars
            PGA = (PGA_UNCONVERTED/100)*9.81
        elif PGA_ScaleFactor == "g":
            PGA = PGA_UNCONVERTED*9.81
        elif PGA_ScaleFactor == "m2/s2":
            PGA = PGA_UNCONVERTED


    # equation for calcs
    if PGA == "":
        Day1EQRate = ""
    else:
        if PGA < YieldAcceleration:
            Day1EQRate = float(BaselineRate)
        else:
            exponent = (C_Hmax * math.log(SlopeHeight_Converted))+(C_alpha *
math.log(SlopeAngle)) + (C_PGA * math.log(PGA)) + C_Intercept
            Day1EQRate = math.exp(exponent)
    return float(Day1EQRate)
"""
# Calculate the field
arcpy.CalculateField_management(inTable, fieldname, expression, "PYTHON3",
codeblock, "FLOAT")

#############################################################################
##################################################################

# 2) Factor of Increase Calcs
# Set variables for field calculations
inTable = Rockslopes_Point_Layer  # table containing the field that will be
updated with the new calculation
fieldname = "IF_EQ"  # field that will be updated (created if it does not
already exist)
expression = "IF_EQ_Function(!PGA!, !PGA_Conv!, !Day1EQRate!)"  # call
calculation function
codeblock = """
def IF_EQ_Function(PGA, PGA_Conv, Day1EQRate):
    BaselineRate = arcpy.GetParameterAsText(1)


    # PGA conversions
    PGA_ScaleFactor = arcpy.GetParameterAsText(2)
    if PGA < 0:
        PGA_UNCONVERTED = float(PGA_Conv)
        PGA = PGA_UNCONVERTED*9.81
    else:
        PGA_UNCONVERTED = float(PGA)

        if PGA_ScaleFactor == "100% g":                     # convert to
proper units for roars
            PGA = (PGA_UNCONVERTED/100)*9.81
        elif PGA_ScaleFactor == "g":
            PGA = PGA_UNCONVERTED*9.81
        elif PGA_ScaleFactor == "m2/s2":
```

```
            PGA = PGA_UNCONVERTED


    # equation for calcs
    if PGA == "":
        IF_EQ = ""
    else:
        IF_EQ = float(Day1EQRate)/float(BaselineRate)
    return float(IF_EQ)
"""
# Calculate the field
arcpy.CalculateField_management(inTable, fieldname, expression, "PYTHON3",
codeblock, "FLOAT")

############################################################################
##################################################################

# 3) EQ Rockfall Volume Calcs
# Set variables for field calculations
inTable = Rockslopes_Point_Layer  # table containing the field that will be
updated with the new calculation
fieldname = "VOL_EQ"  # field that will be updated (created if it does not
already exist)
expression = "VOL_EQ_Function(!PGA!, !PGA_Conv!, !IF_EQ!,
!ESAreaN!,!MSHeigtN!,!MSLengtN!)"  # call calculation function
codeblock = """
def VOL_EQ_Function(PGA, PGA_Conv, IF_EQ, ESAreaN, MSHeigtN, MSLengtN):
    BaselineRate = arcpy.GetParameterAsText(1)

    # unit conversions
    if ESAreaN == None:
        Height = float(MSHeigtN)*0.3048
        Length = float(MSLengtN)*0.3048
        Area = 0.65*Height*Length
    elif ESAreaN == 0:
        Height = float(MSHeigtN)*0.3048
        Length = float(MSLengtN)*0.3048
        Area = 0.65*Height*Length
    else:
        Area = float(ESAreaN)*0.3048*0.3048

    # PGA conversions
    PGA_ScaleFactor = arcpy.GetParameterAsText(2)
    if PGA < 0:
        PGA_UNCONVERTED = float(PGA_Conv)
        PGA = PGA_UNCONVERTED*9.81
    else:
        PGA_UNCONVERTED = float(PGA)

        if PGA_ScaleFactor == "100% g":                     # convert to
proper units for roars
            PGA = (PGA_UNCONVERTED/100)*9.81
        elif PGA_ScaleFactor == "g":
            PGA = PGA_UNCONVERTED*9.81
        elif PGA_ScaleFactor == "m2/s2":
            PGA = PGA_UNCONVERTED
```

```
    # equation for calcs
    if PGA == "":
        VOL_EQ = ""
    else:
        VOL_EQ = float(IF_EQ)*float(BaselineRate)*float(Area)
    return round(float(VOL_EQ),2)
"""
# Calculate the field
arcpy.CalculateField_management(inTable, fieldname, expression, "PYTHON3",
codeblock, "FLOAT")

#
############################################################################
##################################################################

# 4) EQ Rockfall Volume Normalized by length along the slope Calcs
# Set variables for field calculations
inTable = Rockslopes_Point_Layer  # table containing the field that will be
updated with the new calculation
fieldname = "VOL_EQ_div_L"  # field that will be updated (created if it does
not already exist)
expression = "VOL_EQ_div_L_Function(!PGA!, !PGA_Conv!, !MSLengtN!, !VOL_EQ!)"
# call calculation function
codeblock = """
def VOL_EQ_div_L_Function(PGA, PGA_Conv, MSLengtN, VOL_EQ):

    Length = MSLengtN*0.3048

    # PGA conversions
    PGA_ScaleFactor = arcpy.GetParameterAsText(2)
    if PGA < 0:
        PGA_UNCONVERTED = float(PGA_Conv)
        PGA = PGA_UNCONVERTED*9.81
    else:
        PGA_UNCONVERTED = float(PGA)

        if PGA_ScaleFactor == "100% g":                     # convert to
proper units for roars
            PGA = (PGA_UNCONVERTED/100)*9.81
        elif PGA_ScaleFactor == "g":
            PGA = PGA_UNCONVERTED*9.81
        elif PGA_ScaleFactor == "m2/s2":
            PGA = PGA_UNCONVERTED


    # equation for calcs
    if PGA == "":
        VOL_EQ_div_L = ""
    else:
        VOL_EQ_div_L = float(VOL_EQ)/float(Length)
    return round(float(VOL_EQ_div_L),2)
"""
# Calculate the field
arcpy.CalculateField_management(inTable, fieldname, expression, "PYTHON3",
codeblock, "FLOAT")
```

```
#
##############################################################################
####################################################################

# 5) Lower Inc.F Calcs
# Set variables for field calculations
inTable = Rockslopes_Point_Layer  # table containing the field that will be
updated with the new calculation
fieldname = "LOWER_IF_NEQ_Day1"  # field that will be updated (created if it
does not already exist)
expression = "LOWER_IF_NEQ_Day1_Function(!IF_EQ!,!PGA!, !PGA_Conv!)"  # call
calculation function
codeblock = """
def LOWER_IF_NEQ_Day1_Function(IF_EQ, PGA, PGA_Conv):
    # setup
    NEQ_Alpha = 11.823
    NEQ_Beta = 0.4157


    # PGA conversions
    PGA_ScaleFactor = arcpy.GetParameterAsText(2)
    if PGA < 0:
        PGA_UNCONVERTED = float(PGA_Conv)
        PGA = PGA_UNCONVERTED*9.81
    else:
        PGA_UNCONVERTED = float(PGA)

        if PGA_ScaleFactor == "100% g":                     # convert to
proper units for roars
            PGA = (PGA_UNCONVERTED/100)*9.81
        elif PGA_ScaleFactor == "g":
            PGA = PGA_UNCONVERTED*9.81
        elif PGA_ScaleFactor == "m2/s2":
            PGA = PGA_UNCONVERTED


    # equation for calcs
    if PGA == "":
        LOWER_IF_NEQ_Day1 = ""
    else:
        if NEQ_Alpha*(float(IF_EQ)**NEQ_Beta) > float(IF_EQ):
            LOWER_IF_NEQ_Day1 = IF_EQ
        else:
            LOWER_IF_NEQ_Day1 = NEQ_Alpha*(float(IF_EQ)**NEQ_Beta)

    return float(round(LOWER_IF_NEQ_Day1,2))
"""
# Calculate the field
arcpy.CalculateField_management(inTable, fieldname, expression, "PYTHON3",
codeblock, "FLOAT")

#
##############################################################################
####################################################################
```

```
# 6) Lower T_Restore days Calcs
# Set variables for field calculations
inTable = Rockslopes_Point_Layer  # table containing the field that will be
updated with the new calculation
fieldname = "LOWER_T_RESTORE_days"  # field that will be updated (created if
it does not already exist)
expression = "LOWER_T_RESTORE_Function(!LOWER_IF_NEQ_Day1!,!PGA!
,!PGA_Conv!)"  # call calculation function
codeblock = """
def LOWER_T_RESTORE_Function(LOWER_IF_NEQ_Day1, PGA, PGA_Conv):
    # set up
    Decay_Beta = -0.791


    # PGA conversions
    PGA_ScaleFactor = arcpy.GetParameterAsText(2)
    if PGA < 0:
        PGA_UNCONVERTED = float(PGA_Conv)
        PGA = PGA_UNCONVERTED*9.81
    else:
        PGA_UNCONVERTED = float(PGA)

        if PGA_ScaleFactor == "100% g":                         # convert to
proper units for roars
            PGA = (PGA_UNCONVERTED/100)*9.81
        elif PGA_ScaleFactor == "g":
            PGA = PGA_UNCONVERTED*9.81
        elif PGA_ScaleFactor == "m2/s2":
            PGA = PGA_UNCONVERTED


    # equation for calcs
    if PGA == "":
        LOWER_T_RESTORE_days = ""
    else:
        LOWER_T_RESTORE_days = (1/float(LOWER_IF_NEQ_Day1))**(1/Decay_Beta)

    return float(round(LOWER_T_RESTORE_days,2))
"""
# Calculate the field
arcpy.CalculateField_management(inTable, fieldname, expression, "PYTHON3",
codeblock, "FLOAT")

#
#############################################################################
###################################################################

# 7) Lower T_Restore years Calcs
# Set variables for field calculations
inTable = Rockslopes_Point_Layer  # table containing the field that will be
updated with the new calculation
fieldname = "LOWER_T_RESTORE_years"  # field that will be updated (created if
it does not already exist)
expression = "LOWER_T_RESTORE_years_Function(!LOWER_T_RESTORE_days!,!PGA!,
!PGA_Conv!)"  # call calculation function
codeblock = """
```

```
def LOWER_T_RESTORE_years_Function(LOWER_T_RESTORE_days, PGA, PGA_Conv):
    # set up
    Decay_Beta = -0.791


    # PGA conversions
    PGA_ScaleFactor = arcpy.GetParameterAsText(2)
    if PGA < 0:
        PGA_UNCONVERTED = float(PGA_Conv)
        PGA = PGA_UNCONVERTED*9.81
    else:
        PGA_UNCONVERTED = float(PGA)

        if PGA_ScaleFactor == "100% g":                    # convert to 
proper units for roars
            PGA = (PGA_UNCONVERTED/100)*9.81
        elif PGA_ScaleFactor == "g":
            PGA = PGA_UNCONVERTED*9.81
        elif PGA_ScaleFactor == "m2/s2":
            PGA = PGA_UNCONVERTED


    # equation for calcs
    if PGA == "":
        LOWER_T_RESTORE_years = ""
    else:
        LOWER_T_RESTORE_years = int(LOWER_T_RESTORE_days)/365.25

    return round(float((LOWER_T_RESTORE_years)),2)
"""
# Calculate the field
arcpy.CalculateField_management(inTable, fieldname, expression, "PYTHON3", 
codeblock, "FLOAT")

#
############################################################################
##################################################################

# 8) Upper Inc.F Calcs
# Set variables for field calculations
inTable = Rockslopes_Point_Layer  # table containing the field that will be 
updated with the new calculation
fieldname = "UPPER_IF_NEQ_Day1"  # field that will be updated (created if it 
does not already exist)
expression = "UPPER_IF_NEQ_Day1_Function(!IF_EQ!,!PGA!, !PGA_Conv!)"  # call 
calculation function
codeblock = """
def UPPER_IF_NEQ_Day1_Function(IF_EQ, PGA, PGA_Conv):
    # set up
    NEQ_Alpha = 7.575
    NEQ_Beta = 0.3757


    # PGA conversions
    PGA_ScaleFactor = arcpy.GetParameterAsText(2)
    if PGA < 0:
```

```
        PGA_UNCONVERTED = float(PGA_Conv)
        PGA = PGA_UNCONVERTED*9.81
    else:
        PGA_UNCONVERTED = float(PGA)

        if PGA_ScaleFactor == "100% g":                     # convert to
proper units for roars
            PGA = (PGA_UNCONVERTED/100)*9.81
        elif PGA_ScaleFactor == "g":
            PGA = PGA_UNCONVERTED*9.81
        elif PGA_ScaleFactor == "m2/s2":
            PGA = PGA_UNCONVERTED


    # equation for calcs
    if PGA == "":
        UPPER_IF_NEQ_Day1 = ""
    else:
        if NEQ_Alpha*(float(IF_EQ)**NEQ_Beta) > float(IF_EQ):
            UPPER_IF_NEQ_Day1 = IF_EQ
        else:
            UPPER_IF_NEQ_Day1 = NEQ_Alpha*(float(IF_EQ)**NEQ_Beta)

    return round(float(UPPER_IF_NEQ_Day1),2)
"""
# Calculate the field
arcpy.CalculateField_management(inTable, fieldname, expression, "PYTHON3",
codeblock, "FLOAT")

#
##############################################################################
###################################################################

# 9) Upper T_Restore days Calcs
# Set variables for field calculations
inTable = Rockslopes_Point_Layer  # table containing the field that will be
updated with the new calculation
fieldname = "UPPER_T_RESTORE_days"  # field that will be updated (created if
it does not already exist)
expression = "UPPER_T_RESTORE_Function(!UPPER_IF_NEQ_Day1!,!PGA!,
!PGA_Conv!)"  # call calculation function
codeblock = """
def UPPER_T_RESTORE_Function(UPPER_IF_NEQ_Day1, PGA, PGA_Conv):
    # set up
    Decay_Beta = -0.753


    # PGA conversions
    PGA_ScaleFactor = arcpy.GetParameterAsText(2)
    if PGA < 0:
        PGA_UNCONVERTED = float(PGA_Conv)
        PGA = PGA_UNCONVERTED*9.81
    else:
        PGA_UNCONVERTED = float(PGA)

        if PGA_ScaleFactor == "100% g":                     # convert to
```

```
proper units for roars
            PGA = (PGA_UNCONVERTED/100)*9.81
        elif PGA_ScaleFactor == "g":
            PGA = PGA_UNCONVERTED*9.81
        elif PGA_ScaleFactor == "m2/s2":
            PGA = PGA_UNCONVERTED


    # equation for calcs
    if PGA == "":
        UPPER_T_RESTORE_days = ""
    else:
        UPPER_T_RESTORE_days = (1/float(UPPER_IF_NEQ_Day1))**(1/Decay_Beta)

    return round(float(UPPER_T_RESTORE_days),2)
"""
# Calculate the field
arcpy.CalculateField_management(inTable, fieldname, expression, "PYTHON3",
codeblock, "FLOAT")

#
##############################################################################
##################################################################

# 10) Upper T_Restore years Calcs
# Set variables for field calculations
inTable = Rockslopes_Point_Layer  # table containing the field that will be
updated with the new calculation
fieldname = "UPPER_T_RESTORE_years"  # field that will be updated (created if
it does not already exist)
expression = "UPPER_T_RESTORE_years_Function(!UPPER_T_RESTORE_days!,!PGA!,
!PGA_Conv!)"  # call calculation function
codeblock = """
def UPPER_T_RESTORE_years_Function(UPPER_T_RESTORE_days, PGA, PGA_Conv):
    # set up
    Decay_Beta = -0.753


    # PGA conversions
    PGA_ScaleFactor = arcpy.GetParameterAsText(2)
    if PGA < 0:
        PGA_UNCONVERTED = float(PGA_Conv)
        PGA = PGA_UNCONVERTED*9.81
    else:
        PGA_UNCONVERTED = float(PGA)

        if PGA_ScaleFactor == "100% g":                     # convert to
proper units for roars
            PGA = (PGA_UNCONVERTED/100)*9.81
        elif PGA_ScaleFactor == "g":
            PGA = PGA_UNCONVERTED*9.81
        elif PGA_ScaleFactor == "m2/s2":
            PGA = PGA_UNCONVERTED


    # equation for calcs
```

```
    if PGA == "":
        UPPER_T_RESTORE_years = ""
    else:
        UPPER_T_RESTORE_years = float(UPPER_T_RESTORE_days)/365.25

    return round(float((UPPER_T_RESTORE_years)),2)
"""
# Calculate the field
arcpy.CalculateField_management(inTable, fieldname, expression, "PYTHON3",
codeblock, "FLOAT")

#
############################################################################
##################################################################

# 11) Average Inc.F Calcs
# Set variables for field calculations
inTable = Rockslopes_Point_Layer  # table containing the field that will be
updated with the new calculation
fieldname = "AVG_IF_NEQ_Day1"  # field that will be updated (created if it
does not already exist)
expression = "AVG_IF_NEQ_Day1_Function(!IF_EQ!,!PGA!, !PGA_Conv!)"  # call
calculation function
codeblock = """
def AVG_IF_NEQ_Day1_Function(IF_EQ, PGA, PGA_Conv):
    # set up
    NEQ_Alpha = 9.699
    NEQ_Beta = 0.3957


    # PGA conversions
    PGA_ScaleFactor = arcpy.GetParameterAsText(2)
    if PGA < 0:
        PGA_UNCONVERTED = float(PGA_Conv)
        PGA = PGA_UNCONVERTED*9.81
    else:
        PGA_UNCONVERTED = float(PGA)

        if PGA_ScaleFactor == "100% g":                     # convert to
proper units for roars
            PGA = (PGA_UNCONVERTED/100)*9.81
        elif PGA_ScaleFactor == "g":
            PGA = PGA_UNCONVERTED*9.81
        elif PGA_ScaleFactor == "m2/s2":
            PGA = PGA_UNCONVERTED


    # equation for calcs
    if PGA == "":
        AVG_IF_NEQ_Day1 = ""
    else:
        if NEQ_Alpha*(float(IF_EQ)**NEQ_Beta) > float(IF_EQ):
            AVG_IF_NEQ_Day1 = IF_EQ
        else:
            AVG_IF_NEQ_Day1 = NEQ_Alpha*(float(IF_EQ)**NEQ_Beta)
```

```
    return round(float(AVG_IF_NEQ_Day1),2)
"""
# Calculate the field
arcpy.CalculateField_management(inTable, fieldname, expression, "PYTHON3",
codeblock, "FLOAT")

#
##############################################################################
###################################################################

# 12) Average T_Restore days Calcs
# Set variables for field calculations
inTable = Rockslopes_Point_Layer  # table containing the field that will be
updated with the new calculation
fieldname = "AVG_T_RESTORE_days"  # field that will be updated (created if it
does not already exist)
expression = "AVG_T_RESTORE_Function(!AVG_IF_NEQ_Day1!,!PGA!, !PGA_Conv!)"  #
call calculation function
codeblock = """
def AVG_T_RESTORE_Function(AVG_IF_NEQ_Day1, PGA, PGA_Conv):
    # set up
    Decay_Beta = -0.772


    # PGA conversions
    PGA_ScaleFactor = arcpy.GetParameterAsText(2)
    if PGA < 0:
        PGA_UNCONVERTED = float(PGA_Conv)
        PGA = PGA_UNCONVERTED*9.81
    else:
        PGA_UNCONVERTED = float(PGA)

        if PGA_ScaleFactor == "100% g":                     # convert to
proper units for roars
            PGA = (PGA_UNCONVERTED/100)*9.81
        elif PGA_ScaleFactor == "g":
            PGA = PGA_UNCONVERTED*9.81
        elif PGA_ScaleFactor == "m2/s2":
            PGA = PGA_UNCONVERTED


    # equation for calcs
    if PGA == "":
        AVG_T_RESTORE_days = ""
    else:
        AVG_T_RESTORE_days = (1/float(AVG_IF_NEQ_Day1))**(1/Decay_Beta)

    return round(float(AVG_T_RESTORE_days),2)
"""
# Calculate the field
arcpy.CalculateField_management(inTable, fieldname, expression, "PYTHON3",
codeblock, "FLOAT")

#
##############################################################################
###################################################################
```

```
# 13) Average T_Restore years Calcs
# Set variables for field calculations
inTable = Rockslopes_Point_Layer  # table containing the field that will be
updated with the new calculation
fieldname = "AVG_T_RESTORE_years"  # field that will be updated (created if
it does not already exist)
expression = "AVG_T_RESTORE_years_Function(!AVG_T_RESTORE_days!,!PGA!,
!PGA_Conv!)"  # call calculation function
codeblock = """
def AVG_T_RESTORE_years_Function(AVG_T_RESTORE_days, PGA, PGA_Conv):
    # set up
    Decay_Beta = -0.753


    # PGA conversions
    PGA_ScaleFactor = arcpy.GetParameterAsText(2)
    if PGA < 0:
        PGA_UNCONVERTED = float(PGA_Conv)
        PGA = PGA_UNCONVERTED*9.81
    else:
        PGA_UNCONVERTED = float(PGA)

        if PGA_ScaleFactor == "100% g":                     # convert to
proper units for roars
            PGA = (PGA_UNCONVERTED/100)*9.81
        elif PGA_ScaleFactor == "g":
            PGA = PGA_UNCONVERTED*9.81
        elif PGA_ScaleFactor == "m2/s2":
            PGA = PGA_UNCONVERTED


    # equation for calcs
    if PGA == "":
        AVG_T_RESTORE_years = ""
    else:
        AVG_T_RESTORE_years = float(AVG_T_RESTORE_days)/365.25

    return round(float((AVG_T_RESTORE_years)),2)
"""
# Calculate the field
arcpy.CalculateField_management(inTable, fieldname, expression, "PYTHON3",
codeblock, "FLOAT")

#
#############################################################################
###################################################################

# 14) Summary IF_NEQ_Day1 Calcs
# Set variables for field calculations
inTable = Rockslopes_Point_Layer  # table containing the field that will be
updated with the new calculation
fieldname = "SUM_IF_NEQ_Day1"  # field that will be updated (created if it
does not already exist)
expression = "SUM_IF_NEQ_Day1_Function(!AVG_IF_NEQ_Day1!,
!UPPER_IF_NEQ_Day1!, !LOWER_IF_NEQ_Day1!, !PGA!, !PGA_Conv!)"  # call
```

```
calculation function
codeblock = """
def SUM_IF_NEQ_Day1_Function(AVG_IF_NEQ_Day1, UPPER_IF_NEQ_Day1,
LOWER_IF_NEQ_Day1, PGA, PGA_Conv):
    # set up


    # PGA conversions
    PGA_ScaleFactor = arcpy.GetParameterAsText(2)
    if PGA < 0:
        PGA_UNCONVERTED = float(PGA_Conv)
        PGA = PGA_UNCONVERTED*9.81
    else:
        PGA_UNCONVERTED = float(PGA)

        if PGA_ScaleFactor == "100% g":                     # convert to
proper units for roars
            PGA = (PGA_UNCONVERTED/100)*9.81
        elif PGA_ScaleFactor == "g":
            PGA = PGA_UNCONVERTED*9.81
        elif PGA_ScaleFactor == "m2/s2":
            PGA = PGA_UNCONVERTED


    # equation for calcs
    if PGA == "":
        SUM_IF_NEQ_Day1 = ""
    else:
        SUM_IF_NEQ_Day1 = str(str(round(float(AVG_IF_NEQ_Day1)))+"
("+str(round(float(UPPER_IF_NEQ_Day1)))+"-
"+str(round(float(LOWER_IF_NEQ_Day1)))+")")

    return SUM_IF_NEQ_Day1
"""
# Calculate the field
arcpy.CalculateField_management(inTable, fieldname, expression, "PYTHON3",
codeblock, "TEXT")

#
##############################################################################
###################################################################

# 15) Summary T_RESTORE days Calcs
# Set variables for field calculations
inTable = Rockslopes_Point_Layer  # table containing the field that will be
updated with the new calculation
fieldname = "SUM_T_RESTORE_days"  # field that will be updated (created if it
does not already exist)
expression = "SUM_T_RESTORE_days_Function(!AVG_T_RESTORE_days!,
!UPPER_T_RESTORE_days!, !LOWER_T_RESTORE_days!, !PGA!, !PGA_Conv!)"  # call
calculation function
codeblock = """
def SUM_T_RESTORE_days_Function(AVG_T_RESTORE_days, UPPER_T_RESTORE_days,
LOWER_T_RESTORE_days, PGA, PGA_Conv):
    # set up
```

```
    # PGA conversions
    PGA_ScaleFactor = arcpy.GetParameterAsText(2)
    if PGA < 0:
        PGA_UNCONVERTED = float(PGA_Conv)
        PGA = PGA_UNCONVERTED*9.81
    else:
        PGA_UNCONVERTED = float(PGA)

        if PGA_ScaleFactor == "100% g":                     # convert to
proper units for roars
            PGA = (PGA_UNCONVERTED/100)*9.81
        elif PGA_ScaleFactor == "g":
            PGA = PGA_UNCONVERTED*9.81
        elif PGA_ScaleFactor == "m2/s2":
            PGA = PGA_UNCONVERTED


    # equation for calcs
    if PGA == "":
        SUM_T_RESTORE_days = ""
    else:
        SUM_T_RESTORE_days = str(str(round(float(AVG_T_RESTORE_days)))+"
("+str(round(float(UPPER_T_RESTORE_days)))+"-
"+str(round(float(LOWER_T_RESTORE_days)))+")")

    return SUM_T_RESTORE_days
"""
# Calculate the field
arcpy.CalculateField_management(inTable, fieldname, expression, "PYTHON3",
codeblock, "TEXT")

#
############################################################################
##################################################################

# 16) Summary T_RESTORE years Calcs
# Set variables for field calculations
inTable = Rockslopes_Point_Layer  # table containing the field that will be
updated with the new calculation
fieldname = "SUM_T_RESTORE_years"  # field that will be updated (created if
it does not already exist)
expression = "SUM_T_RESTORE_years_Function(!AVG_T_RESTORE_years!,
!UPPER_T_RESTORE_years!, !LOWER_T_RESTORE_years!, !PGA!, !PGA_Conv!)"  # call
calculation function
codeblock = """
def SUM_T_RESTORE_years_Function(AVG_T_RESTORE_years, UPPER_T_RESTORE_years,
LOWER_T_RESTORE_years, PGA, PGA_Conv):
    # set up


    # PGA conversions
    PGA_ScaleFactor = arcpy.GetParameterAsText(2)
    if PGA < 0:
        PGA_UNCONVERTED = float(PGA_Conv)
        PGA = PGA_UNCONVERTED*9.81
```

```
    else:
        PGA_UNCONVERTED = float(PGA)

        if PGA_ScaleFactor == "100% g":                     # convert to
proper units for roars
            PGA = (PGA_UNCONVERTED/100)*9.81
        elif PGA_ScaleFactor == "g":
            PGA = PGA_UNCONVERTED*9.81
        elif PGA_ScaleFactor == "m2/s2":
            PGA = PGA_UNCONVERTED


    # equation for calcs
    if PGA == "":
        SUM_T_RESTORE_years = ""
    else:
        SUM_T_RESTORE_years = str(str(AVG_T_RESTORE_years)+"
("+str(UPPER_T_RESTORE_years)+"-"+str(LOWER_T_RESTORE_years)+")")

    return SUM_T_RESTORE_years
"""
# Calculate the field
arcpy.CalculateField_management(inTable, fieldname, expression, "PYTHON3",
codeblock, "TEXT")

#
##############################################################################
###################################################################

# 17) Closure Time Cost
# Set variables for field calculations
inTable = Rockslopes_Point_Layer  # table containing the field that will be
updated with the new calculation
fieldname = "ClosureTime"  # field that will be updated (created if it does
not already exist)
expression = "ClosureTime_Function(!VOL_EQ!)"  # call calculation function
codeblock = """
def ClosureTime_Function(VOL_EQ):
    Volume = VOL_EQ*1.30795062      # convert to cy
    ClosureTime = 2.9593*(Volume**0.5399)       # output in hours

    return ClosureTime
"""
# Calculate the field
arcpy.CalculateField_management(inTable, fieldname, expression, "PYTHON3",
codeblock, "FLOAT")
```